UNIVERSITY OF CALIFORNIA, SAN DIEGO

Mechanisms of activity-dependent regulation of neurotransmitter switching in the developing and mature nervous system

A dissertation submitted in partial satisfaction of the
requirements for the degree Doctor of Philosophy

in

Biology

by

Da Meng

Committee in charge:

Professor Nicholas C. Spitzer, Chair
Professor Darwin Berg
Professor Stefan Leutgeb
Professor Mark Mayford
Professor Mark Tuszynski

2016

The Dissertation of Da Meng is approved, and it is acceptable in quality and form for publication on microfilm and electronically:

_____

_____

_____

_____

_____

Chair

University of California, San Diego

2016

DEDICATION

To my parents and grandparents,

For encouraging me to pursue the education taken away from them by difficult times

TABLE OF CONTENTS

LIST OF FIGURES

ACKNOWLEDGEMENTS

I would like to thank my doctoral advisor, Dr. Nicholas C. Spitzer, for the tremendous mentorship and guidance throughout my training. Your enthusiasm for pursuing new knowledge and passion for education have had a profound impact on my career. I would like to thank Dr. Darwin Berg for introducing me to the fascinating field of neuroscience as an undergraduate and for your continued encouragement as my committee member. I would also like to thank the rest of my committee, Dr. Stefan Leutgeb, Dr. Mark Mayford, and Dr. Mark Tuszynski for your insightful comments and stimulating discussions. All of your ideas and feedbacks have been absolutely invaluable to my research.

Chapter 1, in full, is a reprint of the material as it appears in Neuron, 2014. Guemez-Gamboa A*, Xu L*, Meng D & Spitzer NC. Neuron. 82(3):501-720. May 7 2014. The dissertation author was a co-author of this paper.

Chapter 2, in full, is currently being prepared for submission for publication of the material. Meng D, Spitzer NC. Neuronal activity regulates transmitter switching in the adult brain. The dissertation author was the primary investigator and author of this material.

VITA

2011 Bachelor of Medicine, Fudan University

2011-2016 Research Assistant, University of California, San Diego

2013-2015 Teaching Assistant, University of California, San Diego

2016 Doctor of Philosophy, University of California, San Diego

ABSTRACT OF THE DISSERTATION

Mechanisms of activity-dependent regulation of neurotransmitter switching in the developing and mature nervous system

by

Da Meng

Doctor of Philosophy in Biology

University of California, San Diego, 2016

Professor Nicholas C. Spitzer, Chair

We are intrigued by how electrical and intracellular calcium activity of neurons can regulate neurotransmitter switching, a newly recognized form neuroplasticity, during development and in the mature nervous system.

In the developing *Xenopus* spinal cord, newly born neurons exhibit characteristic spontaneous calcium activity during a critical period that leads to the specification of distinct neurotransmitter phenotypes, such as glutamate and GABA. Altering electrical and

calcium activity of these spinal neurons in vitro and in vivo causes homeostatic re-specification of neurotransmitters. Here we investigated the molecular mechanism by which neuronal activity regulates transmitter re-specification. We demonstrated that neuronal activity acts non-cell-autonomously through the release of brain-derived neurotrophic factor (BDNF) to regulate a glutamate/GABA selector transcription factor *tlx3* through activation of a TrkB/MAPK signaling pathway.

We then investigated the role of neuronal activity in transmitter switching in the adult mammalian brain. In the adult rat following long-day photoperiod exposure, the number of dopaminergic neurons decreases while the number of somatostatin neurons increases in the paraventricular nucleus of hypothalamus (PaVN), causing anxiety and depression-like behaviors. Here we demonstrated that long-day photoperiod exposure increases neuronal activity of PaVN dopaminergic neurons prior to transmitter switch. Blocking activity of PaVN dopaminergic neurons abolishes their transmitter switch in response to long-day photoperiod exposure, suggesting an activity-dependent cell-population-autonomous mechanism.

CHAPTER 1: Non-cell-autonomous mechanism of activity-dependent neurotransmitter switching in the developing nervous system

Neuron
Article

Non-Cell-Autonomous Mechanism of Activity-Dependent Neurotransmitter Switching

Alicia Guemez-Gamboa,[1,2] Lin Xu,[1,2] Da Meng,[1] and Nicholas C. Spitzer[1,*]
[1]Neurobiology Section, Division of Biological Sciences and Center for Neural Circuits and Behavior, Kavli Institute for Brain and Mind, University of California San Diego, La Jolla, CA 92093-0357, USA
[2]Co-first author
*Correspondence: nspitzer@ucsd.edu
http://dx.doi.org/10.1016/j.neuron.2014.04.029

SUMMARY

Activity-dependent neurotransmitter switching engages genetic programs regulating transmitter synthesis, but the mechanism by which activity is transduced is unknown. We suppressed activity in single neurons in the embryonic spinal cord to determine whether glutamate-gamma-aminobutyric acid (GABA) switching is cell autonomous. Transmitter respecification did not occur, suggesting that it is homeostatically regulated by the level of activity in surrounding neurons. Graded increase in the number of silenced neurons in cultures led to graded decrease in the number of neurons expressing GABA, supporting non-cell-autonomous transmitter switching. We found that brain-derived neurotrophic factor (BDNF) is expressed in the spinal cord during the period of transmitter respecification and that spike activity causes release of BDNF. Activation of TrkB receptors triggers a signaling cascade involving JNK-mediated activation of cJun that regulates *tlx3*, a glutamate/GABA selector gene, accounting for calcium-spike BDNF-dependent transmitter switching. Our findings identify a molecular mechanism for activity-dependent respecification of neurotransmitter phenotype in developing spinal neurons.

INTRODUCTION

Specification of neurotransmitters is a fundamental aspect of neuronal development, allowing establishment of functional connections at synapses and enabling normal operation of the nervous system. Distinct expression patterns of transmitters are initially determined by transcription factors via genetic programs (Cheng et al., 2004; Mizuguchi et al., 2006; Pillai et al., 2007) and subsequently respecified by electrical activity (Dulcis and Spitzer, 2008; Demarque and Spitzer, 2010; Marek et al., 2010). Activity-dependent transmitter respecification is a recently discovered form of brain plasticity, distinct from changes in synaptic strength and number of synapses, in which neurons acquire an additional transmitter, lose a transmitter, or switch between one transmitter and another (Spitzer, 2012). It can be driven by target-derived factors, experimental manipulations of spontaneous activity, or by natural fluctuations in sensory stimuli in both developing and mature neurons (Furshpan et al., 1976; Landis, 1976; Walicke et al., 1977; Schotzinger and Landis, 1988; Gutiérrez, 2002; Borodinsky et al., 2004; Dulcis and Spitzer, 2008; Demarque and Spitzer, 2010; Marek et al., 2010; Dulcis et al., 2013). Spontaneous Ca^{2+} spikes regulate inhibitory and excitatory transmitter phenotypes homeostatically in embryonic *Xenopus* spinal neurons. When Ca^{2+} spikes are suppressed, more neurons express the excitatory neurotransmitters glutamate and acetylcholine. In contrast, when Ca^{2+} spiking is increased, more neurons express the inhibitory neurotransmitters gamma-aminobutyric acid (GABA) and glycine (Borodinsky et al., 2004). Here we identify the signal transduction cascade linking activity to changes in gene expression that lead to transmitter switching.

Electrical activity leads to a wide range of elevations of intracellular Ca^{2+} that could regulate expression of genes determining excitatory or inhibitory phenotype in a cell-autonomous manner. However, these transient elevations of intracellular Ca^{2+} could also regulate cellular secretion enabling inductive interactions among cells to specify neurotransmitter via a non-cell-autonomous mechanism (Spitzer, 2006). The role of cell-autonomous versus non-cell-autonomous mechanisms is often examined in purified and sparsely plated cultures (Tonge and Andrews, 2010), but is more challenging to address in vivo (Lee and Luo, 1999; Zong et al., 2005). We address this issue by developing a single-neuron targeting method in vivo. No transmitter switch was observed in single neurons in which Ca^{2+} spikes had been suppressed, indicating that a non-cell-autonomous mechanism is involved.

Brain-derived neurotrophic factor (BDNF) then became an attractive candidate to regulate activity-dependent transmitter respecification because its expression and release are regulated by neuronal activity (Balkowiec and Katz, 2002; Gärtner and Staiger, 2002; Tabuchi et al., 2000), and it has been implicated in mechanisms that optimize neuronal differentiation and neuronal plasticity (Vicario-Abejón et al., 2002; Park and Poo, 2013). Application or overexpression of BDNF promotes development of inhibition (Ohba et al., 2005), whereas decreased expression or disruption of the function of BDNF impairs development of inhibitory synapses (Hong et al., 2008; Shinoda et al., 2011). On the other hand, application of BDNF leads to suppression of excitatory synaptic transmission (Yang et al., 2002). BDNF exerts its action by binding preferentially to its tyrosine receptor kinase (TrkB) but also through its low-affinity receptor p75. Upon ligand binding, TrkB

receptor dimerization leads to *trans*-autophosphorylation and activation of intracellular signaling cascades, including MAP kinase (MAPK), PI 3-kinase (PI3K), and phospholipase-Cγ (PLCγ) pathways (Huang and Reichardt, 2003).

We demonstrate Ca^{2+} spike-dependent BDNF release, identify critical components of the molecular signaling pathway downstream of BDNF, and show that BDNF regulates glutamate/GABA switching. Thus, genetic programs and collective electrical activity that drives transmitter induction via BDNF determine the mature transmitter phenotype. Understanding the molecular basis of transmitter respecification identifies potential points of intervention for therapeutically enhancing or restoring synaptic transmission that is impaired in neurological or psychiatric disorders.

RESULTS

Suppression of Ca^{2+} Spike Activity in Single Neurons In Vivo

Ca^{2+}-dependent electrical activity in embryonic *Xenopus* spinal neurons homeostatically regulates respecification of the neurotransmitters that neurons express without affecting cell identities both in vivo and in vitro (Borodinsky et al., 2004). Misexpression of human inward rectifier K^+ channels (hKir2.1) by injection of hKir2.1 mRNA causes more neurons to express the excitatory transmitters glutamate and acetylcholine, while fewer neurons express the inhibitory transmitters GABA and glycine in the spinal cord. We developed a single-neuron targeting system to determine whether activity-dependent neurotransmitter respecification is cell autonomous in vivo. Expression from DNA constructs is mosaic and only a few cells express large amounts of transcript whereas most cells express none (Kroll and Amaya, 1996). Accordingly, blastomeres were injected with hKir2.1 DNA instead of mRNA. Although mosaic expression from DNA constructs has been regarded as a nuisance, here it becomes an asset. In addition, neuronal lineages have been determined at the 16-cell stage (Moody, 1989), enabling more specific manipulation of Ca^{2+} spike activity in particular classes of spinal neurons. We thus performed injections at this stage to further limit the number of cells expressing the DNA of interest.

We injected hKir2.1-mCherry DNA into the D1.1 or D1.2 blastomeres of the 16-cell blastula (Figure S1A available online), both of which make a major contribution to neurons in the ventral spinal cord (http://www.xenbase.org). When embryos reached the late tailbud stage (stage 41), mCherry was typically observed in several neurons separated along the spinal cord (Figure S1B), indicating the success of targeting single neurons by this method. Eighty percent were located on the ventral side of the neural tube and only 20% were located on the dorsal side of the neural tube (Figure S1C). Because V1.2 blastomeres make a major contribution to the dorsal spinal cord (http://www.xenbase.org), DNA injection of these cells predominantly targeted neurons on the dorsal side (data not shown).

Activity Blockade in Single Neurons Does Not Switch Neurotransmitters

hKir2.1 has been used to suppress neuronal excitability both in vitro (Burrone et al., 2002) and in vivo (Borodinsky et al., 2004; Mizuno et al., 2007). To determine whether misexpression of hKir2.1-mCherry in single neurons suppresses Ca^{2+} spikes, we assessed Ca^{2+} activity in these mCherry-labeled neurons by confocal imaging of Fluo-4 AM. Although neurons located on both dorsal and ventral surfaces spike in situ in *X. laevis*, those positioned on the dorsal surface spike at lower frequencies at early stages of development (Belgacem and Borodinsky, 2011; Borodinsky et al., 2004; Gu et al., 1994; Root et al., 2008). We thus imaged the intact ventral spinal cord at stage 23-25 when most classes of neurons exhibit a higher incidence and frequency of Ca^{2+} spikes (Borodinsky et al., 2004). Neurons without hKir2.1 expression in the same embryos served as internal controls (Figure 1A). Misexpression of hKir2.1-mCherry decreased both spike incidence and frequency in single neurons (Figures 1B and 1C; Figure S1D). The incidence and frequency of spiking in single neurons expressing mCherry alone were similar to those in internal controls, suggesting that mCherry has no effect on Ca^{2+} spike activity and allows hKir2.1 to effectively exert its hyperpolarizing function (Figure 1C; Figure S1D).

We then determined whether homeostatic transmitter switching occurred in the single neurons in which Ca^{2+} spike activity had been suppressed. The primary nervous system in *Xenopus* embryos is composed of ~1,000 neurons (Hartenstein, 1993). Neurons on the ventral side of the neural tube include cholinergic motor neurons, GABAergic ascending interneurons, and cholinergic/glutamatergic descending interneurons (Li et al., 2004; Roberts et al., 1987). Neurons on the dorsal side of the neural tube comprise the glutamatergic Rohon-Beard sensory neurons and GABAergic/glycinergic dorsolateral ascending interneurons (Roberts et al., 1987; Sillar and Roberts, 1988). If Ca^{2+} spikes acted cell autonomously, we expected that suppressing activity in single neurons on the ventral side of the spinal cord would cause neurons not normally glutamatergic to acquire a glutamatergic phenotype, identified by expression of vesicular glutamate transporter (vGluT1). VGluT1-, but not vGluT2- or vGluT3-immunoreactivity, colocalizes with glutamate immunoreactivity (Glu-IR), making vGluT1 a useful glutamatergic marker (Borodinsky et al., 2004). In parallel, we expected that suppressing activity in single neurons on the dorsal side of the spinal cord would cause them to lose the GABAergic phenotype, assessed by GABA-immunoreactivity (GABA-IR). Neurons were identified by position and morphology. Strikingly, the incidence of vGluT1-IR neurons among hKir2.1-mCherry-labeled ventral neurons and among mCherry-alone-labeled ventral neurons did not differ from each other. This result indicates that the glutamatergic phenotype was not acquired in single neurons in which Ca^{2+} spikes had been suppressed (Figure 1D). Moreover, no difference was observed in the incidence of GABA-IR between hKir2.1-mCherry-labeled neurons and mCherry-alone-labeled dorsal neurons, indicating that there is no decrease in the incidence of GABA-IR cells among the single neurons in which Ca^{2+} spikes have been suppressed (Figure 1E). These data suggest that the mechanism for Ca^{2+} spike activity-dependent transmitter respecification in the embryonic spinal cord is non-cell autonomous.

To further analyze network-dependent regulation of transmitter switching, we changed the ratio of silenced to unsilenced neurons in a graded manner. Because most chemical synapses

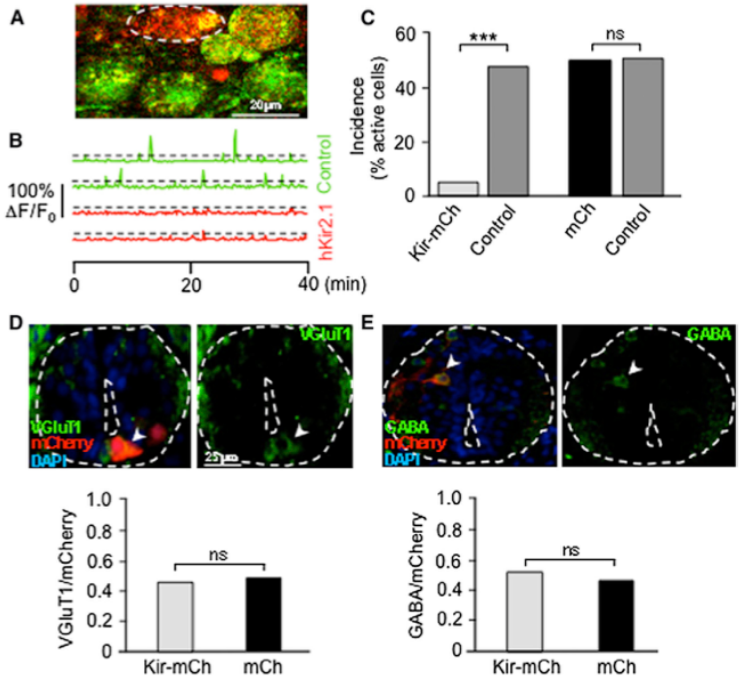

Figure 1. Misexpression of hKir2.1 Suppresses Ca^{2+} Spike Generation in Single Neurons In Situ without Changing the Identity of Their Neurotransmitter

(A) Confocal image of a stage 25 ventral spinal cord. Dashed oval outlines a hKir2.1-mCherry/Fluo-4 AM-expressing neuron (red and yellow). Neurons loaded with Fluo-4 AM (green) are internal controls.

(B) Spike activity is absent in these hKir2.1-mCherry-expressing neurons and present in internal controls. Ca^{2+} spikes were identified as fluorescence transients greater than 20% of $\Delta F/F_0$ (dashed lines), more than twice the SD of the baseline.

(C) Spike incidence during 1 hr imaging periods. $n \geq 7$ stage 23–25 embryos per group; 37–63 neurons were analyzed per group. Kir-mCh cells, hKir2.1-mCherry-expressing neurons; mCh cells, mCherry-expressing neurons.

(D and E) VGluT1 and GABA staining and quantitative analysis of stage 41 larvae from Kir-mCherry DNA- and mCherry DNA-injected embryos. Arrowheads identify a VGluT1-immunoreactive and a GABA-immunoreactive neuron. $n \geq 7$ embryos per group; 36–58 neurons were analyzed for each group. VGluT1/mCherry and GABA/mCherry represent the fraction of mCherry-labeled neurons that are VGluT1-immunoreactive and GABA-immunoreactive.

***$p < 0.001$; ns, not significant with Mann-Whitney U test. See also Figure S1.

have yet to be formed during the period when activity respecifies transmitter identity, the network is likely to involve secreted ligands that diffuse to receptors on neurons. Accordingly, we plated different ratios of active (wild-type) and silenced (hKir2.1-mCherry-labeled) neurons in dissociated cell cultures (Figures 2A and 2B) and assessed the impact of diffusion of agents among synaptically unconnected neurons. The results indicate that the percent of neurons expressing GABA depends on the percent of silenced hKir2.1-mCherry-expressing neurons in the total population, as demonstrated by linear regression analysis (Figure 2C): the slope is significantly nonzero (black). In addition, assuming a linear relationship, the slopes are not significantly different for active (wild-type, gray) and silenced (hKir2.1-mCherry, red) neurons, further supporting a non-cell-autonomous mechanism. We grouped the data into five classes (0%, 25%, 50%, 75%, and 100% of silenced neurons) to determine whether differences in percent of neurons expressing GABA as a function of neurons expressing hKir2.1-mCherry were significant (Figure 2D). We found that increasing the percent of silenced neurons (hKir2.1-mCherry) leads to a progressive decrease in the percent of GABA-IR, further motivating the search for a secreted ligand that regulates neurotransmitter respecification.

BDNF Is Released by Ca^{2+} Spike Activity

Neurotrophins are important regulators of neural development, survival, function, and plasticity (Chao, 2003). Neurotransmitter specification in *Xenopus* embryos is most responsive to changes in Ca^{2+} spike activity during the critical period between neural tube formation (stage 20) and an early larval stage (stage 28); sensitivity decreases and disappears when the embryo approaches stage 35 (Borodinsky et al., 2004; Root et al., 2008). BDNF expression has been detected in the neural plate in *Xenopus* embryos at stage 18 (Huang et al., 2007).

In situ hybridization with a 387 base pair probe to BDNF revealed its expression in the neural plate and neural tube at stages 18, 24, and 28, throughout the critical period for transmitter respecification when spontaneous Ca^{2+} spike activity is present (Figure 3A). TrkB immunostaining identifies the presence of BDNF receptors at stages 24 and 28 (Figure S2), sparsely expressed on a subset of neurons. To determine whether BDNF is released by spike activity, we prepared nerve-muscle cultures from embryos expressing BDNF-pHluorin (Matsuda et al., 2009). Depolarization of neurons with KCl to mimic Ca^{2+} spikes (Gu and Spitzer, 1995) stimulated Ca^{2+}-dependent decreases in fluorescence (Figure 3B). A significant decrease was observed during depolarization in the presence of 2 mM Ca^{2+} (13% ± 1%), whereas no difference was observed during depolarization in the absence of Ca^{2+} (1% ± 2%; Figure 3C). This result is consistent with the changes in BDNF-pHluorin fluorescence observed with substantial BDNF release (Matsuda et al., 2009). To ascertain whether BDNF is released by spontaneous activity throughout this critical period, we collected cell-conditioned culture medium before (1–3 hr in vitro), during (3–9 hr in vitro), and after (14 hr in vitro) spontaneous Ca^{2+} spike activity (Chang and Spitzer, 2009). Only cell-conditioned medium collected during the period of spontaneous Ca^{2+} spike activity showed an increase in the levels of released BDNF compared to the earlier

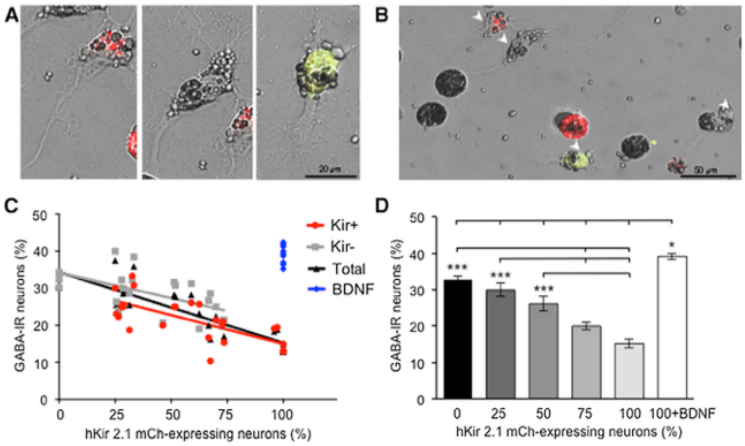

Figure 2. Increasing the Number of Silenced Neurons In Vitro Decreases the Number of Silenced and Active GABA-IR Neurons Equally

(A and B) A representative view of active (wild-type) and silenced (hKir2.1-mCherry labeled) neurons in a dissociated 50% silenced neuron-enriched culture (A). High-magnification views of individual active or silenced neurons (B). Low-magnification view showing two active and two silenced neurons (arrowheads), one of which is GABA-IR+. hKir2.1-mCherry: red; GABA-IR/hKir2.1-mCherry: yellow.

(C) The percent of neurons expressing GABA-IR depends on the percent of silenced neurons expressing hKir2.1-mCherry. Black: total number of GABA-IR neurons/total number of neurons. Red: number of GABA-IR Kir+ neurons/number of Kir+ neurons. Grey: number of GABA-IR Kir− neurons/number of Kir− neurons. Blue: total GABA-IR% of 100% silenced cultures with BDNF addition. Simple linear regression analysis was performed for the first three groups. Total: slope = −0.19 ± 0.02, significantly nonzero ($p < 0.0001$); Kir+: slope = −0.15 ± 0.03, significantly nonzero ($p < 0.0001$); Kir−: slope = −0.14 ± 0.04, significantly nonzero ($p = 0.002$) with use of ANOVA. The slopes for active (Kir−) neurons, silenced (Kir+) neurons, and the total population are not significantly different with use of ANOVA.

(D) Bars represent the percent of neurons expressing GABA-IR from six groups (0%, 25%, 50%, 75%, 100% silenced and 100% silenced plus BDNF). Cultures with more than 35 neurons poststaining were selected, and n = 4–8 cultures per group were analyzed.

Data are mean ± SEM. *$p < 0.05$; ***$p < 0.001$; ****$p < 0.0001$, with use of one-way ANOVA Tukey's multiple comparisons test.

and later times when spontaneous Ca^{2+} spike activity is reduced (Figure 3D). Moreover, a significant increase was observed in cell-conditioned medium from control cultures when compared to cell-conditioned medium obtained from cultures in which Ca^{2+} spike activity had been suppressed by misexpression of hKir2.1 mRNA. These results suggest that BDNF is released in an activity-dependent manner. Strikingly, the decrease in percent of GABA-IR neurons observed after the increase in hKir2.1-mCherry expressing neurons in vitro (Figures 2C and 2D) is prevented when BDNF is applied to cultures of fully silenced neurons. Based on these observations, we hypothesized that BDNF regulates activity-dependent transmitter respecification during early development.

BDNF Regulates Neurotransmitter Phenotype Homeostatically

To examine the role of BDNF in the non-cell-autonomous mechanism of neurotransmitter respecification in vivo, we spatially and temporally restricted production of BDNF by delivering a lissamine-tagged BDNF morpholino (BDNF MO) to the anterior spinal cord by local electroporation at the neural plate stage (stage 15/16) to avoid early developmental defects caused by constitutive inhibition (Figure 4A). Larvae from embryos electroporated with a control MO (CMO) or BDNF MO were fixed at 3 days (stage 41). The number of glutamatergic neurons was increased and the number of GABAergic neurons was decreased in the anterior spinal cord of embryos electroporated with BDNF MO (Figures 4C–4E), mirroring the effect of hKir2.1 misexpression in *Xenopus* spinal neurons on transmitter respecification when Ca^{2+} spike activity is blocked (Borodinsky et al., 2004).

We then implanted small agarose beads adjacent to the anterior spinal cord to locally and chronically release BDNF during specific stages of development (Borodinsky et al., 2004; Root et al., 2008). Beads were loaded with BDNF or vehicle, implanted at the time of neural tube closure (stage 18), and larvae were fixed at stage 41 (Figure 4B). Embryos implanted with BDNF-loaded beads showed an increase in number of GABAergic neurons and a decrease in number of glutamatergic neurons (Figures 4C–4E; Figure S3), mirroring the effect of rat brain sodium channel II (Nav1.2α/β) misexpression in *Xenopus* spinal neurons on transmitter respecification when Ca^{2+} activity is enhanced (Borodinsky et al., 2004).

Activation of the TrkB receptor tyrosine kinase is the principal pathway by which BDNF initiates downstream signaling. To determine whether the observed effect of BDNF on transmitter respecification was mediated by Trk receptors, we delivered K252a, a membrane-permeable tyrosine kinase inhibitor with relatively high affinity for TrkB receptors, via agarose beads implanted in embryos. As a negative control, we implanted embryos with beads containing K252b, the nonfunctional analog of K252a. As expected, the number of GABAergic neurons and glutamatergic neurons in embryos implanted with K252b-loaded beads was similar to that in controls with vehicle-loaded beads. However, Trk inhibition with K252a had a similar effect to that observed following electroporation of the BDNF MO (Figures 4D and 4E; Figure S3), suggesting that BDNF regulates transmitter phenotype through a K252a-sensitive pathway, most likely via TrkB receptor signaling.

To determine whether BDNF is an integration point for Ca^{2+} spike activity-dependent respecification of transmitters, we performed simultaneous manipulations of Ca^{2+} activity and BDNF in vivo. Misexpression of hKir2.1 mRNA to suppress Ca^{2+} spike activity throughout the spinal cord generated an increase in the number of glutamatergic neurons and a decrease in the number of GABAergic neurons. Release of BDNF from beads implanted adjacent to the spinal cord produced the opposite phenotypes.

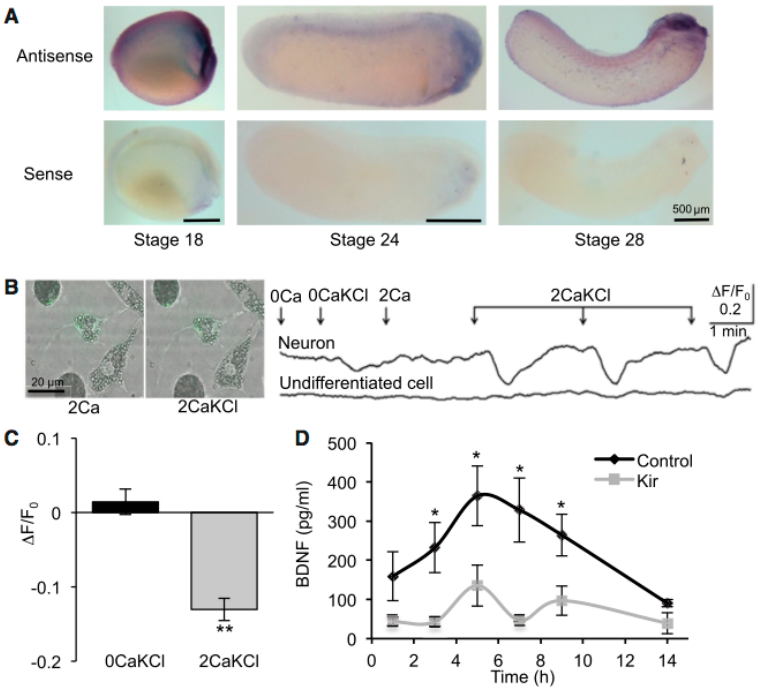

Figure 3. BDNF Is Expressed throughout the Critical Period for Neurotransmitter Specification and Release Depends on Spontaneous Ca^{2+} Spike Activity

(A) BDNF transcript expression in embryos at stages 18, 24, and 28.

(B) BDNF release by Ca^{2+} spike activity. Left: superimposed fluorescence and bright field images of a neuron and muscle and undifferentiated cells loaded with BDNF-pHluorin before and after depolarization with 2 mM Ca^{2+} + 100 mM KCl (2CaKCl). Right: representative trace showing time course of cell body fluorescence changes of a neuron and an undifferentiated cell. The culture was first depolarized with KCl in the absence of Ca^{2+} as control (0CaKCl), and then depolarized three times in the presence of Ca^{2+} (2CaKCl). Each 30 s depolarization, mimicking a Ca^{2+} spike, causes a decrease in BDNF-pHluorin fluorescence selectively in the neuron in the presence of Ca^{2+}. Arrows indicate the start of perfusion: 0Ca, 0 mM Ca^{2+} + 0.67 mM KCl; 0CaKCl, 0 mM Ca^{2+} + 100 mM KCl; 2Ca, 2 mM Ca^{2+} + 0.67 mM KCl; and 2CaKCl, 2 mM Ca^{2+} + 100 mM KCl.

(C) Quantification of the decrease of BDNF-pHluorin fluorescence in response to 2CaKCl. n = 5 neurons from five independent experiments. Data are mean ± SEM. **p < 0.01 with use of Mann-Whitney U test.

(D) BDNF protein in culture medium in the absence (Kir) or in the presence (control) of spontaneous activity. Cultures were prepared from embryos injected either with hKir2.1 mRNA and cascade blue dextran or cascade blue dextran (control). Medium was collected at the indicated times and released BDNF levels (pg/ml) were measured with a conventional two-site ELISA system. n ≥ 4 cultures per condition; ≥ 40 neurons/culture. Kir, hKir2.1 misexpression. Data are mean ± SEM. *p < 0.05 with use of Mann-Whitney U test.

Simultaneous suppression of Ca^{2+} activity and application of BDNF in the spinal cord phenocopied the result obtained by application of BDNF alone (Figures 4F and 4G). These results indicate that Ca^{2+} spike activity regulates transmitter specification upstream of BDNF function. Given the low frequency and apparently stochastic generation of Ca^{2+} spikes, the non-cell-autonomous coordination of Ca^{2+} spike activity and BDNF derived from neighboring neurons may drive transmitter switching more reliably than cell-autonomous Ca^{2+} spike activity alone.

BDNF Regulates Neurotransmitter Fate via JNK-Mediated cJun Phosphorylation

We next investigated the intracellular pathway regulated by BDNF. Previous work identified cJun phosphorylation as the Ca^{2+} spike entry point in the genetic pathway (Marek et al., 2010). Because Ca^{2+} activity regulates phosphorylation of cJun and BDNF is downstream of Ca^{2+} spikes, we first determined whether BDNF regulates phosphorylation of cJun in vitro. Western blotting of extracts from neuronal cultures with phospho-specific antibodies showed that phosphorylation of cJun (P-cJun) at serine 73 (S73) was decreased in response to Ca^{2+} spike suppression or in the absence of Ca^{2+} but was restored after BDNF application. In addition, K252a but not K252b blocked the effect of Ca^{2+} spikes on cJun phosphorylation (Figure 5A), and immunostaining of the embryonic spinal cord (stage 28) revealed that TrkB is expressed in the same subset of neurons showing cJun phosphorylation (Figure 5B), suggesting that BDNF-induced cJun phosphorylation is mediated by TrkB receptor signaling.

To confirm these results in vivo, we examined S73 cJun phosphorylation after BDNF manipulation. Embryos were electroporated with BDNF MO at the neural plate stage (stage 15/16) or implanted with BDNF-loaded beads at the time of neural tube closure (stage 18), fixed at 1.5 days of age (stage 28), sectioned, and immunostained. BDNF-treated embryos showed an increase in the number of cells exhibiting cJun phosphorylation (14% to 28% of total cells expressing cJun), whereas the opposite effect was found when BDNF function was knocked down by morpholino electroporation (14% to 7% of total cells expressing cJun; Figure 5C). This result is consistent with the previous demonstration of decreased phosphorylation of cJun in response to Ca^{2+} spike suppression and increased phosphorylation in response to Ca^{2+} spike enhancement (Marek et al., 2010). No changes were observed in the number of cells expressing cJun (Figure 5D).

To identify the signaling components downstream of BDNF leading to changes in cJun phosphorylation, we turned again to neuronal cultures. A pharmacological screen was used to determine which drugs reduce the level of phosphorylated cJun detected by western blots of protein extracts from neuronal cultures in which Ca^{2+} activity is present. BDNF stimulates

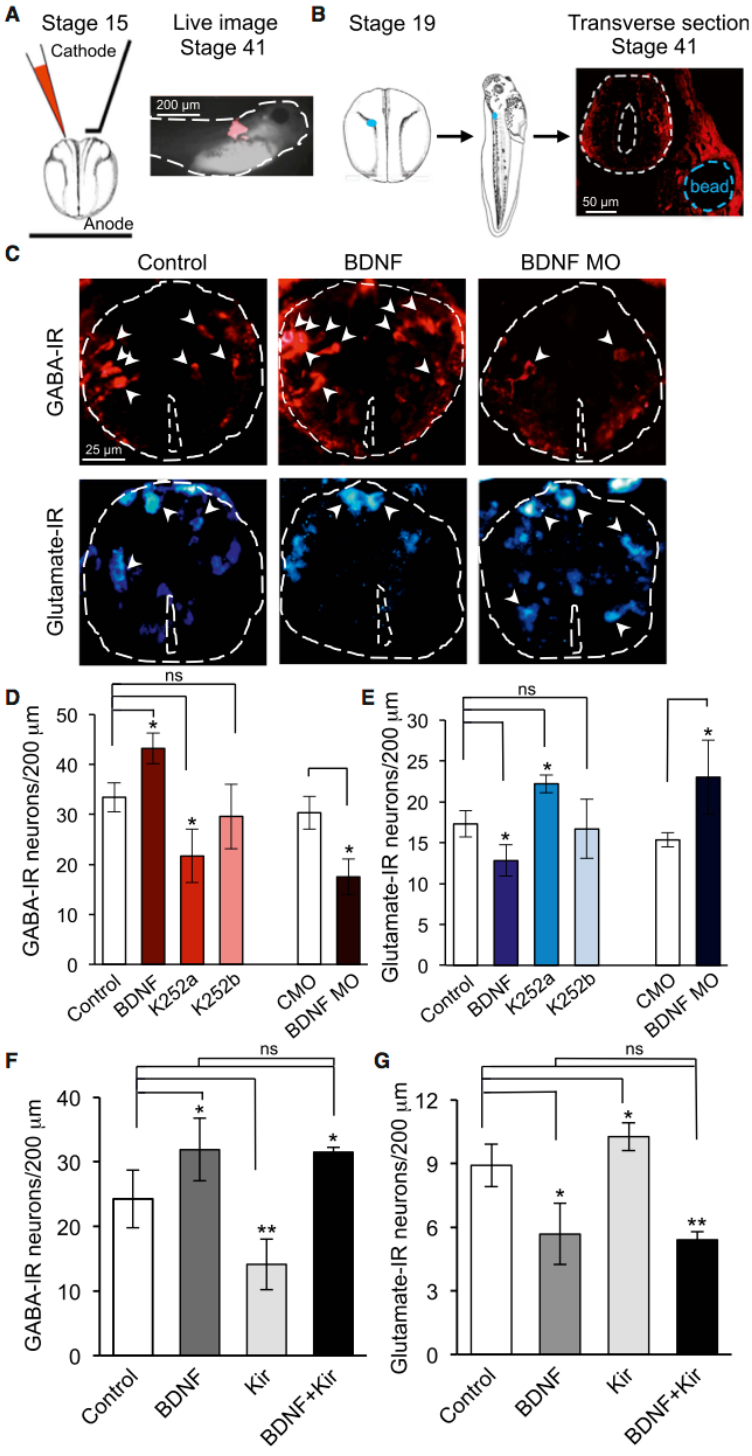

Figure 4. BDNF Regulates Neurotransmitter Phenotype Downstream of Ca^{2+} Spike Activity

(A) Embryos were electroporated with lissamine-tagged BDNF MO or CMO. Lissamine distribution (red) in a live stage 41 larva demonstrates targeting of the spinal cord.

(B) Single agarose beads (blue) loaded with BDNF, K252a, or K252b were implanted adjacent to the nascent neural tube (white dashed circle) at stage 19 and stage 41 larvae were sectioned for immunocytochemistry.

(C–E) GABA (C and D) and glutamate (C and E) staining following implantation of beads containing BDNF (100 ng/ml), K252a or K252b (50 µM), a membrane-impermeable analog of K252a, or BDNF MO and CMO electroporation. Beads were located adjacent to the most rostral 100 µm of the spinal cord; $n \geq 5$ embryos per condition; 101–195 neurons were analyzed per condition per 200 µm.

(F and G) GABA and glutamate expression in embryos in the presence of BDNF (C–E), in embryos misexpressing hKir2.1, and in embryos misxpressing hKir2.1 in the presence of BDNF. $n \geq 5$ embryos per condition; 128–255 neurons were analyzed per condition per 200 µm.

Data are mean ± SEM. *$p < 0.05$; **$p < 0.01$. ns, not significant. ANOVA test with Bonferroni post hoc analysis was used. See also Figure S2.

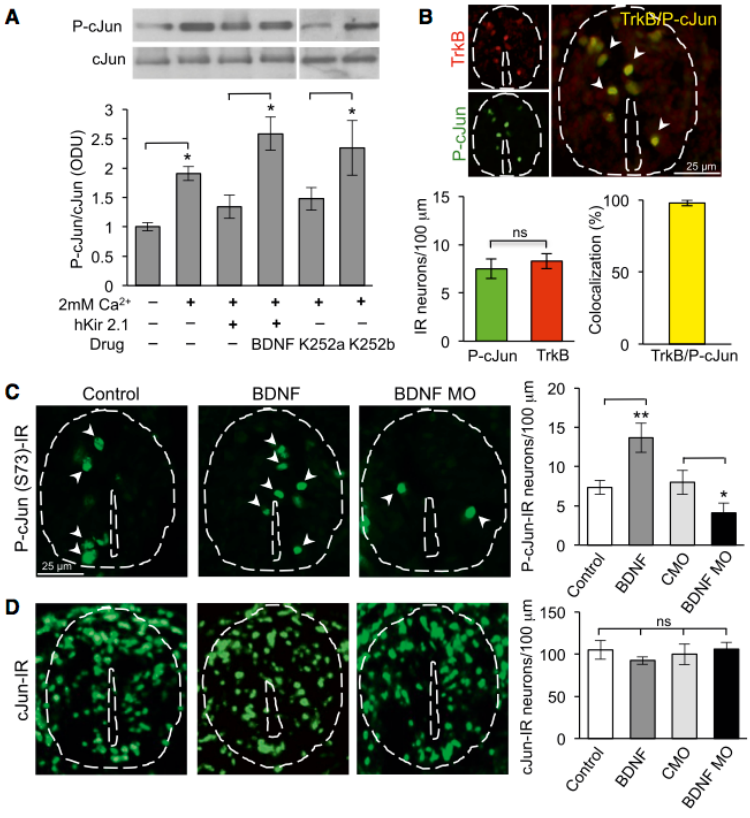

Figure 5. BDNF Regulates cJun Phosphorylation

(A) P-cJun expression in the presence or absence of hKir2.1 expression, BDNF (100 ng/ml) or Trk receptor blocker (50 µM). Protein levels in neuronal cultures were determined by western blot. Graph presents the ratio between the phosphorylated protein and total protein expressed in optical density units (ODU). n ≥ 5 cultures per condition. Kir, hKir2.1 misexpression. Full-length western blot is shown in Figure S5.

(B) P-cJun and TrkB staining of embryos (stage 28) showing colocalization. n ≥ 5 embryos per condition; 132–151 neurons were analyzed per condition per 100 µm.

(C and D) P-cJun (C) and cJun (D) staining of embryos (stage 28) in the presence of control or BDNF beads or electroporated with BDNF MO or CMO. n ≥ 5 embryos per condition; 137–158 neurons were analyzed per condition per 100 µm. Data are mean ± SEM. *p < 0.05; **p < 0.01 with use of Mann-Whitney U test.

pathways regulated by MAPK, PI3K, and PLCγ by activation of TrkB receptors (Huang and Reichardt, 2003). We first assessed the role of MAPK inhibitors to characterize the kinase that phosphorylates cJun. cJun can be phosphorylated by MAPKs such as JNK, p38, and ERK1/2. Accordingly, we used SP600125 to inhibit JNK, U0126 to inhibit ERK1/2 (MEK), and SB235699 to inhibit p38. Western blot assays demonstrated that inhibiting JNK and MEK, but not p38, causes a significant decrease in cJun phosphorylation (Figure S4).

Because Ca^{2+} activity could be involved, we tested inhibitors for the Ca^{2+}-dependent kinases PKC (GF109203x) and CAMKII (KN-93). To determine whether TrkB/MAPK signaling is the principal pathway responsible for cJun phosphorylation, we tested inhibitors for the PI3K (LY294002) and PLCγ (U73122) pathways. Western blot assay showed that phosphorylation of cJun was not decreased in response to any of these inhibitors (Figure S4), suggesting that the TrkB-activated MAPK signaling pathway is responsible for cJun phosphorylation.

To further test the participation of MAPK in BDNF signaling, we performed western blot assays on cultures following Ca^{2+} spike suppression and BDNF addition. Both MEK and JNK inhibitors reduced cJun phosphorylation mediated by BDNF (Figure 6A). JNK is an attractive candidate because it can regulate cJun activity via direct phosphorylation of cJun S63/S73 and T91/T93 (Raivich, 2008) and its expression has been detected in the head and the dorsal region of stage 24 embryos by both RT-PCR and in situ hybridization (Yamanaka et al., 2002).

To determine whether BDNF activates JNK in vivo to phosphorylate cJun, we examined JNK phosphorylation after BDNF manipulation. Embryos were electroporated with the BDNF MO or implanted with BDNF-loaded beads, in separate experiments, fixed at stage 28, sectioned, and immunostained to examine JNK activation. BDNF-treated embryos showed an increase in the number of cells exhibiting JNK phosphorylation whereas the opposite effect was found when BDNF function was knocked down by MO electroporation (Figure 6B), suggesting that the BDNF-induced signaling pathway leads to JNK activation. No changes were observed in the number of cells expressing JNK (Figure 6C). Consistent with western blot results, in vivo electroporation of a JNK MO blocked the increases in P-cJun-IR (Figure 7A), mimicking the effect of the BDNF MO described above and suggesting that JNK has a primary role in the BDNF-induced signaling pathway leading to cJun phosphorylation. No changes were observed in the number of cells expressing cJun (Figure 7B). Moreover, the JNK MO blocked the increase in GABA-IR and the decrease in glutamate-IR otherwise stimulated by misexpression of Nav1.2α/β that increases Ca^{2+} spike activity (Figures 7C and 7D). Thus, BDNF regulates transmitter respecification by modulating JNK-mediated cJun phosphorylation via a TrkB/MAPK signaling pathway.

DISCUSSION

Regulation of the levels of an existing neurotransmitter has been well characterized, but the molecular signaling involved in

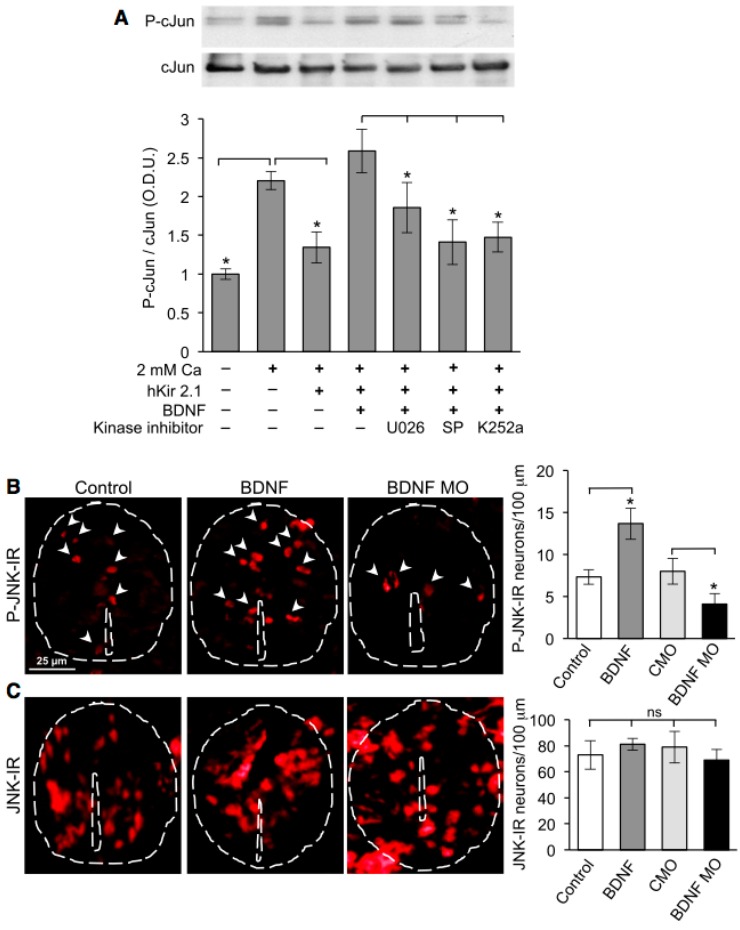

Figure 6. Signaling Pathway Regulating BDNF-Dependent cJun Phosphorylation

(A) P-cJun expression in the presence or absence of BDNF (100 ng/ml) and inhibitors of ERK1/2 (MEK, U0126), JNK (SP600125), or Trk receptors (K252a; all 10 μM). Graph as in Figure 5. n ≥ 5 cultures per condition; ≥ 40 neurons/culture. Data are mean ± SEM. *p < 0.05 with use of ANOVA test with Bonferroni post hoc analysis. Full-length western blot is shown in Figure S5.

(B and C) P-JNK (B) and JNK (C) staining of embryos in the presence of control or BDNF beads or electroporated with BDNF MO or CMO. n ≥ 5 stage 28 embryos per condition; 137–151 neurons were analyzed per condition per 100 μm. Data are mean ± SEM. *p < 0.05 with use of Mann-Whitney U test.

transmitter respecification initiated by activity has received little attention. Increases or decreases in Ca^{2+} spike activity during development of the *Xenopus* nervous system lead to changes in transmitter specification that are generally compensatory and homeostatic. Here we have developed a practical method to manipulate Ca^{2+} activity in single neurons in vivo to determine whether changes are triggered by alteration of activity in single neurons. Our results indicate that suppression of activity in single spinal neurons is not sufficient to trigger changes in transmitters, identifying the role of a non-cell-autonomous mechanism. Graded suppression of activity in an increasingly large fraction of a neuronal population led to a graded change in the number of neurons expressing GABA, with no difference between silenced and active neurons. We then demonstrated that Ca^{2+} spike activity generated prior to synapse formation acts via BDNF through a TrkB/MAPK signaling pathway to phosphorylate cJun and respecify transmitter phenotype. These results identify a molecular cascade that transduces electrical activity into a switch in transmitter identity.

Silencing Single Neurons In Vivo and Graded Populations In Vitro

Although delivery of genes to single cells in vivo is conceptually and experimentally attractive, it has been challenging to implement due to technical difficulties. Single-cell gene targeting is useful to determine whether the effects induced by exogenous or endogenous gene expression in the targeted cell are cell autonomous or due to interactions with neighboring cells. In *Drosophila,* homozygous mutant cells have been targeted for mosaic analysis by placing a repressible cell marker (MARCM) in *trans* to a mutant gene of interest using FLP/FRT-mediated mitotic recombination (Lee and Luo, 1999). In mice, the Cre/loxP system has been applied to develop a method for mosaic analysis with double markers for simultaneous labeling and mutation of neurons (Zong et al., 2005). These genetic methods are efficient in labeling small populations of neurons and even single cells in small or inaccessible embryos when blastomere injection is not an option.

Ca^{2+} spike frequency homeostatically regulates respecification of transmitters in the spinal cord during a brief critical period (Borodinsky et al., 2004; Root et al., 2008). The number of neurons in which transmitter switching occurs is modest, both because the number of primary neurons is small (Hartenstein, 1993) and because some neurons do not demonstrate transmitter respecification (Borodinsky et al., 2004; Dulcis and Spitzer, 2008; Dulcis et al., 2013). We determined whether the effect on transmitter switching induced by Ca^{2+} spike activity occurs via a cell-autonomous mechanism by targeting single neurons efficiently with foreign gene (hKir2.1) expression in *Xenopus* at early developmental stages. Injection of this DNA into specific blastomeres of 16-cell-stage embryos drives its expression in a mosaic pattern in spinal neurons and suppresses spike activity in these neurons. Suppression of Ca^{2+} spikes in single neurons

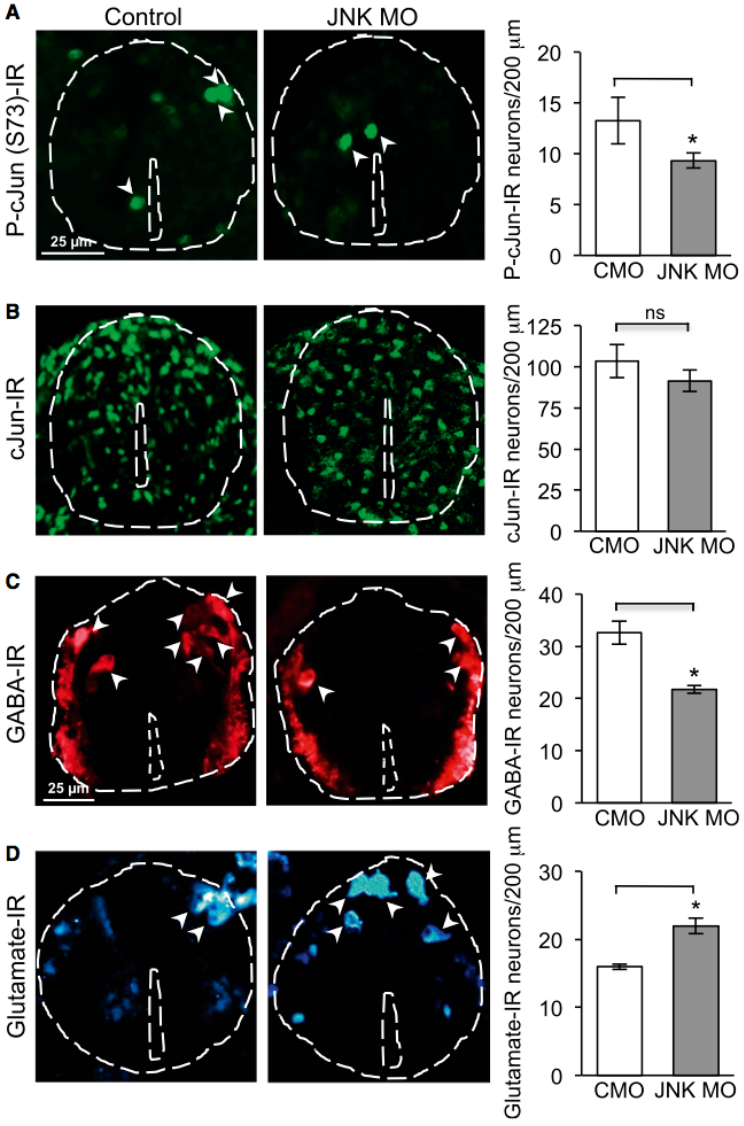

Figure 7. JNK Regulates cJun Phosphorylation and Neurotransmitter Phenotype

(A and B) P-cJun (A) and cJun (B) staining of embryos (stage 28) electroporated with JNK MO or CMO; 128–152 neurons were analyzed per condition per 100 µm.

(C and D) GABA (C) and glutamate (D) staining of embryos (stage 41) following JNK MO and CMO electroporation. n ≥ 5 embryos per condition; 152–215 neurons were analyzed per condition per 200 µm.

Data are mean ± SEM. *p < 0.05 with use of Mann-Whitney U test.

did not result in an increase in incidence of glutamate expression or a decrease in the incidence of GABA expression, providing evidence for non-cell-autonomous regulation. The absence of transmitter switching is unlikely to be due to delay of the normal process, because it was assayed well beyond the end of the critical period, when neurotransmitter in each subtype of neuron has been determined (Root et al., 2008). Cholinergic motorneurons demonstrate coactivity across the spinal cord at these early stages, enabling motorneurons on a silenced half of the spinal cord to receive excitation from motorneurons on an unsilenced half of the spinal cord, consistent with the observation that only bilateral and not unilateral silencing of activity is sufficient to switch the cholinergic phenotype (Borodinsky et al., 2004). However, synchronized activity does not appear to be a general feature of these differentiating neurons. In contrast, glutamatergic and GABAergic neurons, which lack comparable synaptic excitation at this stage of development, exhibit transmitter switching in a silenced half of the spinal cord (Borodinsky et al., 2004).

Consistent with this result, a progressive increase in the percent of silenced neurons in culture leads to a progressive decrease in the percent of neurons expressing GABA, equally in active and in silenced neurons. Thus, the transmitter switches observed following global spike suppression in the entire spinal cord result from a non-cell-autonomous process. A key determinant appears to be the activity of surrounding neurons, rather than the activity level of the target neuron itself.

Role of BDNF in Balancing Neurotransmitter Specification

BDNF appears to be a differentiation factor for most neurons (Park and Poo, 2013). It stimulates formation and maturation of inhibitory GABAergic neurons and synapses (Ohba et al., 2005) and suppresses excitatory synaptic transmission (Yang et al., 2002). Adult glutamatergic hippocampal granule cells in culture coexpress a GABAergic phenotype when incubated in the presence of BDNF (Gómez-Lira et al., 2005). BDNF increases the number and density of GABAergic synapses in solitary neurons cultured from rat visual cortex (Palizvan et al., 2004) and in hippocampal neurons in vivo (Shinoda et al., 2011). Exogenous BDNF prevents the enhancement of synaptic strengths normally induced by chronic blockage of activity in cortical cultures. Furthermore, preventing activation of endogenous BDNF receptors mimics the effects of activity blockade and increases synaptic strengths (Rutherford et al., 1998).

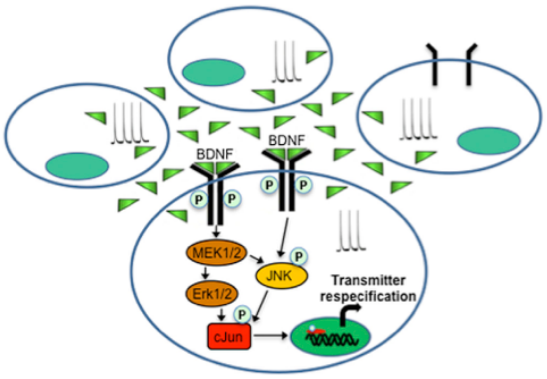

Figure 8. Model of Non-Cell-Autonomous Regulation of Transmitter Expression

Transmitter identity is initially specified genetically and then modulated by environmental influences through changes in spontaneous Ca^{2+}-dependent activity. Ca^{2+} spikes regulate the release of BDNF that initiates the TrkB/MAPK signaling cascade. JNK-mediated phosphorylation of cJun regulates transcription to select neurotransmitter fate.

Our results indicate that BDNF is released from neurons in a Ca^{2+} spike activity-dependent manner and that BDNF regulates activity-dependent transmitter respecification. GFAP immunoreactivity is detected in radial cells in the neural tube as early as stage 24 (Szaro and Gainer, 1988) and GFAP-positive cells can express BDNF (Dreyfus et al., 1999; Abe et al., 2010); further studies will be needed to determine whether glia release BDNF in an activity-dependent or independent manner. An activity-independent BDNF source may be responsible for the release of BDNF observed after activity suppression. Activity-dependent release of BDNF increased the number of GABAergic neurons in the spinal cord in agreement with demonstration that BDNF scales up inhibitory neuronal networks; it decreased the number of glutamatergic neurons consistent with scaling down excitatory neuronal networks.

BDNF Signaling in Ca^{2+} Activity-Dependent Neurotransmitter Switching

BDNF appears to regulate transmitter respecification via TrkB receptors, because the effects of a BDNF MO and K252a on the incidence of glutamatergic and GABAergic neurons were indistinguishable. The sparse expression of TrkB receptors, on a subset of cells, is consistent with transmitter switching in a subset of neurons. Interestingly, the neurons expressing TrkB receptors are the same neurons presenting the activated cJun pathway. They are distributed throughout the spinal cord and do not appear to constitute a previously identified class of neurons. BDNF could stimulate PLCγ, PI3K, and MAPK signaling pathways via activation of TrkB receptors (Huang and Reichardt, 2003). However, we found that the MAPK pathway, but not the PI3K or the PLC-γ pathways, regulated the phosphorylation of cJun by BDNF via MEK and JNK. BDNF preferentially activates MEK but may also activate JNK (Chao, 2003) and there is cross-talk between these two signaling pathways (Dong and Bode, 2003). JNK regulates cJun activity via direct phosphorylation of S63/S73 and T91/T93 (Raivich, 2008) and MEK can also phosphorylate cJun S63/S73 via ERK 1/2 (Morton et al., 2003). Both MEK and JNK signaling had a role in cJun phosphorylation; whether they act in series or in parallel pathways remains to be determined. BDNF caused an increase in JNK phosphorylation that was correlated with an increase in cJun activation, because both the JNK MO and BDNF MO decreased cJun phosphorylation similarly. The number of P-cJun-IR neurons is small at each time point but it is likely that the total number is larger. Because the data are snapshots in time, they do not reveal the total number of neurons showing P-cJun during the period of Ca^{2+} spiking. P-cJun acts as a Ca^{2+} spike-dependent repressor of the homeobox gene *tlx3* that functions as a switch specifying the glutamatergic over GABAergic phenotype in *Xenopus* (Marek et al., 2010). Consistent with this action, the percentage of neurons expressing P-cJun is similar to the percentage of GABAergic neurons in the absence or presence of BDNF, suggesting that they are linked. Direct double staining of P-cJun and GABA or glutamate is not possible because the former has disappeared by the time the latter appears. The JNK MO mimicked the effect of the BDNF MO on the numbers of P-cJun-, GABA-, and glutamate-IR neurons, suggesting that JNK signaling pathway activation is sufficient to phosphorylate cJun and lead to BDNF-induced transmitter switching. Determination of the molecular cascade by which activity drives transmitter respecification is essential for development of the tools with which to gain control over transmitter changes.

Model for Non-Cell-Autonomous Regulation of Transmitter Switching

Neuronal activity plays an important role in regulating many properties of neurons, including neuronal migration and synaptic plasticity, either cell autonomously (Burrone et al., 2002; Tong et al., 2009) or non-cell autonomously (Hartman et al., 2006; Wright and Ribera, 2010). We propose a model for non-cell-autonomous Ca^{2+} spike activity-mediated homeostatic transmitter respecification in *Xenopus* spinal neurons during early stages of development (Figure 8). Transmitter identity is initially specified genetically and then modulated by environmental influences through changes in spontaneous Ca^{2+}-dependent activity. Ca^{2+} spikes regulate the release of BDNF that initiates the TrkB/MAPK signaling cascade. This cascade involves JNK-mediated phosphorylation of cJun that regulates *tlx3* transcription through a CRE site in its promoter (Marek et al., 2010). Parallel pathways may be involved to ensure that the correct transmitter phenotype is established and maintained throughout development. The integration of activity and genetic programs provides a better understanding of transmitter switching and may also provide insights into the pathogenesis of neurological disorders, such as depression, to which environmental stimuli contribute and in which transmitter expression is altered.

EXPERIMENTAL PROCEDURES

Detailed experimental procedures are provided in the Supplemental Experimental Procedures. All animal procedures were performed in accordance

with institutional guidelines and approved by the UCSD Institutional Animal Care and Use Committee.

Blastomere Injection

DNA injection (1 nl of 0.2 mg/ml hKir2.1-mCherry-pcDNA3.1 or mCherry-pcDNA3.1) was performed at the 16-cell stage in specific blastomeres identified according to Moody (1989). RNA injection (5–10 nl of 0.01–0.1 mg/ml hKir2.1 or BDNF-pHluorin with 10,000 molecular weight 20 mg/ml cascade blue dextran) was performed at either the 2- or 16-cell stage. Injections were accomplished using a picospritzer (Picospritzer III, Parker Instrumentation).

Calcium Imaging

Stage 23–25 embryos were dissected as previously described (Gu et al., 1994). Briefly, neural tubes were pinned to expose the ventral surface and loaded for 45 min with 5 μM of the Fluo-4 AM Ca^{2+} indicator (Invitrogen) and 0.01% Pluronic F-127 detergent (Invitrogen) in 2 mM Ca^{2+} saline. Images were acquired at 0.2 Hz for 1 hr periods with a Leica SP5 confocal system and Ca^{2+} transients were scored as spikes when the rise time was complete within 5 s and the amplitude exceeded 20% of $\Delta F/F_0$, more than twice the standard deviation of the baseline during the previous 10 min. Seven to ten embryos were imaged for each experiment. All hKir2.1-mCherry- or mCherry-expressing single neurons from these embryos were analyzed. Neurons not expressing hKir2.1-mCherry or mCherry in the same embryos were internal controls. The incidence of spiking neurons from each experimental group was calculated by dividing the number of neurons that spiked at least once during the 1 hr imaging period by the total number of neurons analyzed in that group.

Immunocytochemistry

Immunocytochemistry was performed as previously described (Borodinsky et al., 2004; Marek et al., 2010). Further information is provided in the Supplemental Experimental Procedures.

Cell Culture

Neuron-enriched cultures were prepared from the posterior neural plate of stage 15 *X. laevis* embryos as previously described (Gu et al., 1994). Details can be found in the Supplemental Experimental Procedures.

Graded Expression of Activity

Embryos were injected with 0.6 mg/ml hKir2.1-mCherry mRNA at the one- or two-cell stage and neuron-enriched cultures were prepared at stage 15 with 0%, 25%, 50%, 75%, or 100% silenced neurons. Graded silencing was achieved by mixing cells from neural plates of embryos expressing hKir2.1 differentially. For example, 75% silencing was achieved by plating half of a neural plate from an embryo expressing hKir2.1 unilaterally with half of a neural plate from an embryo expressing hKir2.1 bilaterally. For the rescue experiment, recombinant BDNF (100 ng/ml, Chemicon Millipore) was added to cultures with 100% silenced neurons. Cultures were fixed with 4% paraformaldehyde with 0.1% glutaraldehyde at 1 day in vitro and immunostained for GABA. Cultures with more than 35 neurons poststaining were selected and the percentages of neurons singly and doubly labeled for GABA-IR and hKir2.1-mCherry were scored.

Whole Mount In Situ Hybridization

Whole mount in situ hybridization was performed (Harland, 1991) using antisense and sense probes generated from pX112-13 containing a partial *Xenopus* BDNF cDNA (a generous gift from Dr. Susana Cohen-Cory, UC Irvine). Details are provided in the Supplemental Experimental Procedures.

Time-Lapse Imaging of BDNF-pHluorin

Ca^{2+} spike-dependent BDNF release was assayed in cultures prepared from embryos injected with BDNF-phluorin mRNA at the 16-cell stage and grown in 0 mM Ca^{2+} medium for 9–12 hr. Cultures were mounted in a custom-made chamber, perfused with salines containing 100 mM KCl in the absence or presence of 2 mM Ca^{2+} for 30 s to mimic Ca^{2+} spikes as previously described (Gu and Spitzer, 1995), and imaged on a Leica SP5 confocal microscope with 63× water-immersion objective. Time-lapse images were acquired at 1.29 s intervals. Cell body fluorescence intensity of BDNF-pHluorin-expressing neurons was quantified using ImageJ and normalized by nonneuronal cells in the same fields.

BDNF Immunoassay

BDNF released under different conditions was measured with a conventional two-site ELISA system according to the manufacturer's protocol (Promega).

Morpholino Electroporation

Local electroporation was performed on stage 15/16 embryos, ~18 hr post-fertilization, using a protocol based on the method developed by Sasagawa et al. (2002). Embryos were placed on an agarose bed over a circular platinum anode (20 mm in diameter; NEPA GENE) in a 1× Marc's Modified Ringer's solution to decrease the resistance between the two electrodes. We targeted the region of interest identified by a map of presumptive spinal cord region of the neural tube of stage 15 embryos (Eagleson and Harris, 1990) with the BDNF MO, JNK MO, or a control MO. Morpholino solutions (5 nl of 0.25 μg/μl) were injected into the presumptive spinal cord region of the closing neural tube. A platinum wire cathode (0.5 mm diameter; Sigma) was placed over the region of interest immediately after injection and a Grass stimulator was used to deliver six square pulses of 5 ms, 40 V, at 500 ms intervals. Electroporated embryos were transferred to 10% Marc's Modified Ringer's solution and maintained at 18°C to slow development, promote healing, and allow a longer period of action. Nonelectroporated embryos grown in the same conditions served as controls. Larvae with lissamine fluorescence extending over a region of 400 μm encompassing the anterior spinal cord were analyzed at stage 41, approximately 5 days after electroporation.

Pharmacology

Agarose beads (100–200 mesh, Bio-Rad) were loaded overnight with drugs (50 μM K252a, K252b; 100 ng/μl BDNF) or DMSO/H_2O (control) and inserted between the neural tube and myotomes at 20 hr of development (stage 18; Borodinsky et al., 2004; Root et al., 2008). Sections of embryos with beads located adjacent to the first 100 μm of the spinal cord were collected 2 days later (stage 41). Changes in both GABA and glutamate expression in spinal neurons were significant along all 400 μm of the rostral spinal cord in K252a bead-implanted embryos, consistent with the small size of K252a (0.4 kD) enabling diffusion. Changes in both GABA and glutamate expression were significant only over the first 100 μm from the BDNF-loaded bead, consistent with limited diffusion of recombinant BDNF (27 kD). Stock concentrations of kinase inhibitors SP600125, SB235699, U0126, KN-93, GF 109203x, LY294002, and U73122 (Tocris Bioscience) were 10 mM in DMSO and were added to the culture medium as indicated. Stock concentrations of drugs were 1 mM K252a (Sigma-Aldrich) and 1 mM K252b (Sigma-Aldrich) in DMSO, and 1 mg/ml recombinant BDNF (Millipore) in distilled water.

Statistics

Means and SEMs were calculated using Microsoft Excel. Statistical analyses were performed using STATA. For comparisons among more than two groups, the ANOVA test was used and followed by Bonferroni post hoc test. For comparisons between two groups, the Mann-Whitney U test was used. Values were considered as significantly different at $p < 0.05$.

SUPPLEMENTAL INFORMATION

Supplemental Information includes Supplemental Experimental Procedures and five figures and can be found with this article online at http://dx.doi.org/10.1016/j.neuron.2014.04.029.

AUTHOR CONTRIBUTIONS

L.X., A.G., D.M., and N.C.S. designed the experiments; L.X., A.G., and D.M. performed the experiments and analysis; and L.X., A.G., D.M., and N.C.S. wrote and edited the manuscript.

ACKNOWLEDGMENTS

We thank Armando de la Torre for technical assistance and Dr. Darcy Kelley for facilities and support. We are grateful to Drs. Darwin Berg, Andrew Huberman, and Yimin Zou for insightful comments on an earlier draft of the manuscript. This work was supported by NIH NS15918 and NS57690.

Accepted: April 14, 2014
Published: June 4, 2014

REFERENCES

Abe, M., Kimoto, H., Eto, R., Sasaki, T., Kato, H., Kasahara, J., and Araki, T. (2010). Postnatal development of neurons, interneurons and glial cells in the substantia nigra of mice. Cell. Mol. Neurobiol. *30*, 917–928.

Balkowiec, A., and Katz, D.M. (2002). Cellular mechanisms regulating activity-dependent release of native brain-derived neurotrophic factor from hippocampal neurons. J. Neurosci. *22*, 10399–10407.

Belgacem, Y.H., and Borodinsky, L.N. (2011). Sonic hedgehog signaling is decoded by calcium spike activity in the developing spinal cord. Proc. Natl. Acad. Sci. USA *108*, 4482–4487.

Borodinsky, L.N., Root, C.M., Cronin, J.A., Sann, S.B., Gu, X., and Spitzer, N.C. (2004). Activity-dependent homeostatic specification of transmitter expression in embryonic neurons. Nature *429*, 523–530.

Burrone, J., O'Byrne, M., and Murthy, V.N. (2002). Multiple forms of synaptic plasticity triggered by selective suppression of activity in individual neurons. Nature *420*, 414–418.

Chang, L.W., and Spitzer, N.C. (2009). Spontaneous calcium spike activity in embryonic spinal neurons is regulated by developmental expression of the Na+, K+-ATPase beta3 subunit. J. Neurosci. *29*, 7877–7885.

Chao, M.V. (2003). Neurotrophins and their receptors: a convergence point for many signalling pathways. Nat. Rev. Neurosci. *4*, 299–309.

Cheng, L., Arata, A., Mizuguchi, R., Qian, Y., Karunaratne, A., Gray, P.A., Arata, S., Shirasawa, S., Bouchard, M., Luo, P., et al. (2004). Tlx3 and Tlx1 are post-mitotic selector genes determining glutamatergic over GABAergic cell fates. Nat. Neurosci. *7*, 510–517.

Demarque, M., and Spitzer, N.C. (2010). Activity-dependent expression of Lmx1b regulates specification of serotonergic neurons modulating swimming behavior. Neuron *67*, 321–334.

Dong, Z., and Bode, A.M. (2003). Dialogue between ERKs and JNKs: friendly or antagonistic? Mol. Interv. *3*, 306–308.

Dreyfus, C.F., Dai, X., Lercher, L.D., Racey, B.R., Friedman, W.J., and Black, I.B. (1999). Expression of neurotrophins in the adult spinal cord *in vivo*. J. Neurosci. Res. *56*, 1–7.

Dulcis, D., and Spitzer, N.C. (2008). Illumination controls differentiation of dopamine neurons regulating behaviour. Nature *456*, 195–201.

Dulcis, D., Jamshidi, P., Leutgeb, S., and Spitzer, N.C. (2013). Neurotransmitter switching in the adult brain regulates behavior. Science *340*, 449–453.

Eagleson, G.W., and Harris, W.A. (1990). Mapping of the presumptive brain regions in the neural plate of *Xenopus laevis*. J. Neurobiol. *21*, 427–440.

Furshpan, E.J., MacLeish, P.R., O'Lague, P.H., and Potter, D.D. (1976). Chemical transmission between rat sympathetic neurons and cardiac myocytes developing in microcultures: evidence for cholinergic, adrenergic, and dual-function neurons. Proc. Natl. Acad. Sci. USA *73*, 4225–4229.

Gärtner, A., and Staiger, V. (2002). Neurotrophin secretion from hippocampal neurons evoked by long-term-potentiation-inducing electrical stimulation patterns. Proc. Natl. Acad. Sci. USA *99*, 6386–6391.

Gómez-Lira, G., Lamas, M., Romo-Parra, H., and Gutiérrez, R. (2005). Programmed and induced phenotype of the hippocampal granule cells. J. Neurosci. *25*, 6939–6946.

Gu, X., and Spitzer, N.C. (1995). Distinct aspects of neuronal differentiation encoded by frequency of spontaneous Ca^{2+} transients. Nature *375*, 784–787.

Gu, X., Olson, E.C., and Spitzer, N.C. (1994). Spontaneous neuronal calcium spikes and waves during early differentiation. J. Neurosci. *14*, 6325–6335.

Gutiérrez, R. (2002). Activity-dependent expression of simultaneous glutamatergic and GABAergic neurotransmission from the mossy fibers in vitro. J. Neurophysiol. *87*, 2562–2570.

Harland, R.M. (1991). In situ hybridization: an improved whole-mount method for *Xenopus* embryos. Methods Cell Biol. *36*, 685–695.

Hartenstein, V. (1993). Early pattern of neuronal differentiation in the Xenopus embryonic brainstem and spinal cord. J. Comp. Neurol. *328*, 213–231.

Hartman, K.N., Pal, S.K., Burrone, J., and Murthy, V.N. (2006). Activity-dependent regulation of inhibitory synaptic transmission in hippocampal neurons. Nat. Neurosci. *9*, 642–649.

Hong, E.J., McCord, A.E., and Greenberg, M.E. (2008). A biological function for the neuronal activity-dependent component of BDNF transcription in the development of cortical inhibition. Neuron *60*, 610–624.

Huang, E.J., and Reichardt, L.F. (2003). Trk receptors: roles in neuronal signal transduction. Annu. Rev. Biochem. *72*, 609–642.

Huang, J.K., Dorey, K., Ishibashi, S., and Amaya, E. (2007). BDNF promotes target innervation of *Xenopus* mandibular trigeminal axons in vivo. BMC Dev. Biol. *7*, 59.

Kroll, K.L., and Amaya, E. (1996). Transgenic *Xenopus* embryos from sperm nuclear transplantations reveal FGF signaling requirements during gastrulation. Development *122*, 3173–3183.

Landis, S.C. (1976). Rat sympathetic neurons and cardiac myocytes developing in microcultures: correlation of the fine structure of endings with neurotransmitter function in single neurons. Proc. Natl. Acad. Sci. USA *73*, 4220–4224.

Lee, T., and Luo, L. (1999). Mosaic analysis with a repressible cell marker for studies of gene function in neuronal morphogenesis. Neuron *22*, 451–461.

Li, W.C., Soffe, S.R., and Roberts, A. (2004). Glutamate and acetylcholine corelease at developing synapses. Proc. Natl. Acad. Sci. USA *101*, 15488–15493.

Marek, K.W., Kurtz, L.M., and Spitzer, N.C. (2010). cJun integrates calcium activity and tlx3 expression to regulate neurotransmitter specification. Nat. Neurosci. *13*, 944–950.

Matsuda, N., Lu, H., Fukata, Y., Noritake, J., Gao, H., Mukherjee, S., Nemoto, T., Fukata, M., and Poo, M.M. (2009). Differential activity-dependent secretion of brain-derived neurotrophic factor from axon and dendrite. J. Neurosci. *29*, 14185–14198.

Mizuguchi, R., Kriks, S., Cordes, R., Gossler, A., Ma, Q., and Goulding, M. (2006). Ascl1 and Gsh1/2 control inhibitory and excitatory cell fate in spinal sensory interneurons. Nat. Neurosci. *9*, 770–778.

Mizuno, H., Hirano, T., and Tagawa, Y. (2007). Evidence for activity-dependent cortical wiring: formation of interhemispheric connections in neonatal mouse visual cortex requires projection neuron activity. J. Neurosci. *27*, 6760–6770.

Moody, S.A. (1989). Quantitative lineage analysis of the origin of frog primary motor and sensory neurons from cleavage stage blastomeres. J. Neurosci. *9*, 2919–2930.

Morton, S., Davis, R.J., McLaren, A., and Cohen, P. (2003). A reinvestigation of the multisite phosphorylation of the transcription factor c-Jun. EMBO J. *22*, 3876–3886.

Ohba, S., Ikeda, T., Ikegaya, Y., Nishiyama, N., Matsuki, N., and Yamada, M.K. (2005). BDNF locally potentiates GABAergic presynaptic machineries: target-selective circuit inhibition. Cereb. Cortex *15*, 291–298.

Palizvan, M.R., Sohya, K., Kohara, K., Maruyama, A., Yasuda, H., Kimura, F., and Tsumoto, T. (2004). Brain-derived neurotrophic factor increases inhibitory synapses, revealed in solitary neurons cultured from rat visual cortex. Neuroscience *126*, 955–966.

Park, H., and Poo, M.M. (2013). Neurotrophin regulation of neural circuit development and function. Nat. Rev. Neurosci. *14*, 7–23.

Pillai, A., Mansouri, A., Behringer, R., Westphal, H., and Goulding, M. (2007). Lhx1 and Lhx5 maintain the inhibitory-neurotransmitter status of interneurons in the dorsal spinal cord. Development *134*, 357–366.

Raivich, G. (2008). c-Jun expression, activation and function in neural cell death, inflammation and repair. J. Neurochem. *107*, 898–906.

Roberts, A., Dale, N., Ottersen, O.P., and Storm-Mathisen, J. (1987). The early development of neurons with GABA immunoreactivity in the CNS of *Xenopus laevis* embryos. J. Comp. Neurol. *261*, 435–449.

Root, C.M., Velázquez-Ulloa, N.A., Monsalve, G.C., Minakova, E., and Spitzer, N.C. (2008). Embryonically expressed GABA and glutamate drive electrical activity regulating neurotransmitter specification. J. Neurosci. *28*, 4777–4784.

Rutherford, L.C., Nelson, S.B., and Turrigiano, G.G. (1998). BDNF has opposite effects on the quantal amplitude of pyramidal neuron and interneuron excitatory synapses. Neuron *21*, 521–530.

Sasagawa, S., Takabatake, T., Takabatake, Y., Muramatsu, T., and Takeshima, K. (2002). Improved mRNA electroporation method for *Xenopus* neurula embryos. Genesis *33*, 81–85.

Schotzinger, R.J., and Landis, S.C. (1988). Cholinergic phenotype developed by noradrenergic sympathetic neurons after innervation of a novel cholinergic target in vivo. Nature *335*, 637–639.

Shinoda, Y., Sadakata, T., Nakao, K., Katoh-Semba, R., Kinameri, E., Furuya, A., Yanagawa, Y., Hirase, H., and Furuichi, T. (2011). Calcium-dependent activator protein for secretion 2 (CAPS2) promotes BDNF secretion and is critical for the development of GABAergic interneuron network. Proc. Natl. Acad. Sci. USA *108*, 373–378.

Sillar, K.T., and Roberts, A. (1988). Unmyelinated cutaneous afferent neurons activate two types of excitatory amino acid receptor in the spinal cord of *Xenopus laevis* embryos. J. Neurosci. *8*, 1350–1360.

Spitzer, N.C. (2006). Electrical activity in early neuronal development. Nature *444*, 707–712.

Spitzer, N.C. (2012). Activity-dependent neurotransmitter respecification. Nat. Rev. Neurosci. *13*, 94–106.

Szaro, B.G., and Gainer, H. (1988). Immunocytochemical identification of non-neuronal intermediate filament proteins in the developing *Xenopus laevis* nervous system. Brain Res. *471*, 207–224.

Tabuchi, A., Nakaoka, R., Amano, K., Yukimine, M., Andoh, T., Kuraishi, Y., and Tsuda, M. (2000). Differential activation of brain-derived neurotrophic factor gene promoters I and III by Ca^{2+} signals evoked via L-type voltage-dependent and N-methyl-D-aspartate receptor Ca^{2+} channels. J. Biol. Chem. *275*, 17269–17275.

Tong, X.P., Li, X.Y., Zhou, B., Shen, W., Zhang, Z.J., Xu, T.L., and Duan, S. (2009). $Ca^{(2+)}$ signaling evoked by activation of $Na^{(+)}$ channels and $Na^{(+)}/Ca^{(2+)}$ exchangers is required for GABA-induced NG2 cell migration. J. Cell Biol. *186*, 113–128.

Tonge, P.D., and Andrews, P.W. (2010). Retinoic acid directs neuronal differentiation of human pluripotent stem cell lines in a non-cell-autonomous manner. Differentiation *80*, 20–30.

Vicario-Abejón, C., Owens, D., McKay, R., and Segal, M. (2002). Role of neurotrophins in central synapse formation and stabilization. Nat. Rev. Neurosci. *3*, 965–974.

Walicke, P.A., Campenot, R.B., and Patterson, P.H. (1977). Determination of transmitter function by neuronal activity. Proc. Natl. Acad. Sci. USA *74*, 5767–5771.

Wright, M.A., and Ribera, A.B. (2010). Brain-derived neurotrophic factor mediates non-cell-autonomous regulation of sensory neuron position and identity. J. Neurosci. *30*, 14513–14521.

Yamanaka, H., Moriguchi, T., Masuyama, N., Kusakabe, M., Hanafusa, H., Takada, R., Takada, S., and Nishida, E. (2002). JNK functions in the non-canonical Wnt pathway to regulate convergent extension movements in vertebrates. EMBO Rep. *3*, 69–75.

Yang, B., Slonimsky, J.D., and Birren, S.J. (2002). A rapid switch in sympathetic neurotransmitter release properties mediated by the p75 receptor. Nat. Neurosci. *5*, 539–545.

Zong, H., Espinosa, J.S., Su, H.H., Muzumdar, M.D., and Luo, L. (2005). Mosaic analysis with double markers in mice. Cell *121*, 479–492.

Acknowledgement

Chapter 1, in full, is a reprint of the material as it appears in Neuron, 2014. Guemez-Gamboa A*, Xu L*, Meng D & Spitzer NC. Neuron. 82(3):501-720. May 7 2014. The dissertation author was a co-author of this paper.

CHAPTER 2: Neuronal activity regulates neurotransmitter switching in the adult brain

SUMMARY

Neurotransmitter switching in the adult mammalian brain has recently been demonstrated in the hypothalamus of the adult rat following altered photoperiod exposure. However, whether the mechanism is activity-dependent is unknown. Here we demonstrated elevated overall neuronal activity and activity of dopaminergic neurons in the paraventricular nucleus of hypothalamus (PaVN) prior to transmitter switching. We then suppressed activity of PaVN dopaminergic neurons with genetic and viral tools and showed that it is sufficient to block their transmitter switching after long-day photoperiod, suggesting a cell-population-autonomous mechanism for transmitter switching. PaVN dopaminergic neurons co-express vesicular glutamate transporter 2 both at the mRNA and protein levels. Suppressing activity of PaVN glutamatergic neurons decreases the number of PaVN dopaminergic neurons. The effect is not mimicked by suppressing activity of all PaVN neurons.

INTRODUCTION

Our nervous system is constantly challenged by changes in endogenous activity and the external environment. By modulating its function through various forms of neuronal plasticity, the brain encodes new information while maintaining a homeostatic balance (Marder and Goaillard, 2006). By incorporating new experience into existing neural circuitry, neuroplasticity underlies important aspects of cognitive function such as learning

and memory, and regulation of social and emotional behaviors such as affection, fear and anxiety (Davidson and McEwen, 2012; Hill and Martinowich, 2016).

Individual neurons within neuronal circuits communicate through the release of neurotransmitters at synapses. Although many aspects of synaptic connections have been shown to be plastic and modulated by neural activity, such as changes in synaptic strength and synapse number (Engert and Bonhoeffer, 1999; Destexhe and Marder, 2004; Turrigiano, 2008), the identity of the neurotransmitters expressed in different neurons has been thought to be fixed and unchanging. The idea has been that the identity of transmitters expressed by neurons is determined by genetic machinery during development and remains the same throughout the lifetime of the organism.

However, accumulating evidence now demonstrates transmitter switching, including transmitter loss, addition, or replacement, both in the developing and mature nervous system in vitro and in vivo (Spitzer, 2015). Moreover, neuronal activity has been shown to play an essential role in neurotransmitter switching in the developing nervous system: Ca^{2+} spikes regulate transmitter respecification of glutamate and GABA non-cell-autonomously by the release of BDNF in the developing *Xenopus* spinal cord. Suppressing neuronal activity by either removing calcium from cell culture medium or expressing inwardly rectifying potassium channels (Kir) in all spinal neurons increased the number of neurons expressing excitatory neurotransmitters glutamate and acetylcholine and decreased the number of neurons expressing inhibitory neurotransmitters GABA and glycine in the spinal cord. Enhancing neuronal activity caused the opposite changes (Gu and Spitzer, 1995; Borodinsky et al., 2004; Guemez-Gamboa et al., 2014).

In the mature nervous system, activity-dependent neuroplasticity has been shown to be involved in stress-related disorders (Christoffel et al., 2011). Activation of the hypothalamic-pituitary-adrenal (HPA) axis by corticotropin-releasing factor (CRF) is the common stress response pathway. The paraventricular nucleus of the hypothalamus (PaVN) integrates stress-relevant signals from multiple brain regions and regulates CRF release through several classic neuroplasticity-related mechanisms, including changing the amount of glutamate released on CRF neurons after a single action potential and the number of glutamatergic synapses on CRF neurons (Bains et al., 2015). Additionally, recent work from our lab demonstrated that neurotransmitter switching in the PaVN is involved in the light-induced stress response as well. Exposing adult rats to a long-day photoperiod (19 hours continuous light and 5 hours continuous dark per day, 19L:5D) decreases the number of dopaminergic neurons and increases the number of somatostatin neurons in the PaVN compared to the numbers following exposure to a balanced-day photoperiod (12L:12D). This transmitter switch leads to an elevated CRF level in the plasma and to anxious and depressive behaviors (Dulcis et al., 2013).

Given the activity-dependence of transmitter switching observed in the developing nervous system, we asked what the role of electrical activity is in transmitter switching in the adult rat brain, using long-day photoperiod-induced transmitter switching in the PaVN as our model. We have now investigated the changes in neuronal activity of different neuronal populations in the PaVN following photoperiod exposures, manipulated neuronal activity with viral and genetic tools, and examined the effects on transmitter switching in PaVN dopaminergic neurons.

RESULTS

Long-day photoperiod exposure increases PaVN neuronal activity prior to transmitter switching

The suprachiasmatic nucleus (SCN) receives direct photic input from retinal ganglion cells reflecting changes in environmental light-dark cycle, and retinorecipient SCN neurons in turn send efferent projections to distinct nuclei in the hypothalamus including the PaVN (Buijs et al., 1993; Vrang et al., 1995b; Munch et al., 2002). Here we examined how PaVN neuronal activity would change in response to long-day photoperiod exposure, using c-Fos as a marker for neuronal activation (Bullitt, 1990). A 77% increase in the number of c-Fos+ cells was observed in the PaVN after 4 days of long-day photoperiod exposure (19L:5D) compared to balanced-day photoperiod (12L:12D) (Figure 1A,B), indicating an elevation of overall PaVN neuronal activity. In addition, co-expression of c-Fos and tyrosine hydroxylase (TH), a marker for dopaminergic neurons, was examined. We found a 63% increase in the number of neurons expressing both TH and c-Fos after 19L:5D compared to 12L:12D (Figure 1A,C), indicating that the activity of PaVN dopaminergic neurons increased after 4 days exposure to the long-day photoperiod. Neurotransmitter switching in the PaVN and subsequent behavioral changes were detected only after one week of altered photoperiod exposure (Dulcis et al., 2013). Therefore, elevation in overall PaVN neuronal activity and the activity of PaVN dopaminergic neurons occurred prior to detectable transmitter switching.

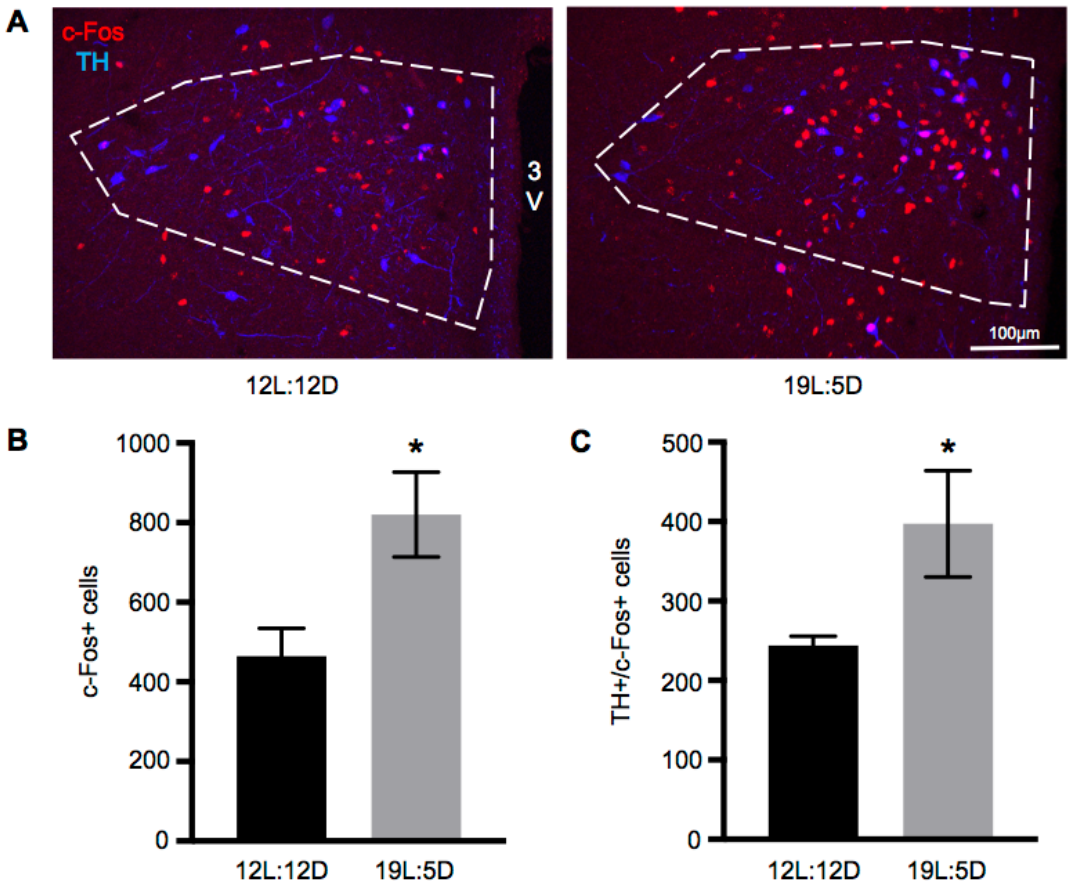

Figure 2.1: 19L:5D long-day photoperiod exposure increases PaVN neuronal activity prior to transmitter switching. WT rats were exposed to either long-day photoperiod (19L:5D) or balanced-day photoperiod (12L:12D) for 4 days. Immunofluorescent staining of TH and c-Fos was performed with fixed brain sections. (A) Confocal images of rat PaVN with TH in blue and c-Fos in red. White dashed line indicates the boundary of the PaVN. 3V, third ventricle. (B) Quantification of the number of c-Fos+ cells in the PaVN per animal. n=6 animals per group. Data are mean ± SEM. *, $p<0.05$. Welch's t test. (C) Quantification of the number of TH+/c-Fos+ cells in the PaVN per animal. n=6 animals per group. Data are mean ± SEM. *, $p<0.05$. Welch's t test.

Suppressing activity of PaVN dopaminergic neurons blocks transmitter switching after 19L:5D without changing TH expression after 12L:12D

To investigate the role of elevated PaVN neuronal activity in regulating transmitter switching, we suppressed the activity of PaVN dopaminergic neurons specifically using TH-Cre transgenic rats stereotaxically injected with a Cre-dependent AAV virus expressing inwardly rectifying potassium channels (AAV-DIO-Kir). By hyperpolarizing infected neurons, Kir has been shown to inhibit action potentials and elevations of intracellular Ca^{2+} effectively (Kubo et al., 1993; Guemez-Gamboa et al., 2014). AAV-DIO-EYFP was used as control. Four weeks after viral injection, to allow sufficient viral expression, the rats were exposed to 19L:5D or 12L:12D for 2 weeks. We first examined whether suppressing electrical activity of PaVN dopaminergic neurons changes their TH expression following exposure to the balanced-day photoperiod. There is no difference in the number of TH+ neurons between the Kir and EYFP groups after 12L:12D (Figure 2A,C), indicating that suppressing activity of PaVN dopaminergic neurons does not change their TH expression during balanced-day photoperiod. Moreover, after a 2-week exposure to 19L:5D, there was a significant decrease in the number of TH+ neurons in the control group (Figure 2B,C), replicating the result of transmitter switching from our previous study. This decrease in the number of TH+ neurons was abolished in the Kir group after long-day photoperiod exposure (Figure 2B,C), indicating that suppressing electrical activity of PaVN dopaminergic neurons is sufficient to block the transmitter switch elicited by exposure to the 19L:5D photoperiod.

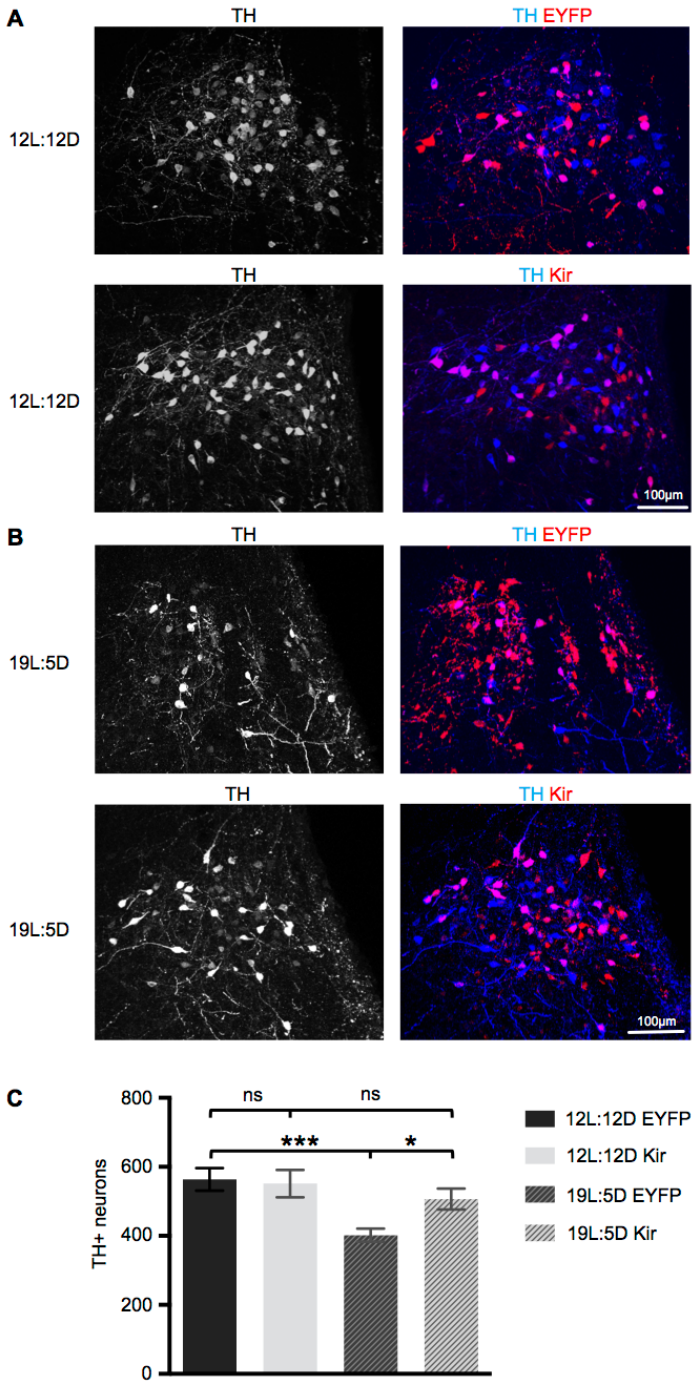

Figure 2.2: Suppressing activity of PaVN dopaminergic neurons blocks transmitter switching after 19L:5D exposure without changing their TH expression after 12L:12D. TH-Cre rats were injected with AAV-DIO-hKir2.1 virus in the PaVN and then exposed to either 12L:12D or 19L:5D for 2 weeks. TH-Cre rats injected with AAV-DIO-EYFP virus were used as controls. Immunofluorescent staining of TH was performed. (A-B) Confocal images showing PaVN TH expression (left) and the expression of TH and viruses (right) after 12L:12D (A) or 19L:5D (B). (C) Quantification of the number of PaVN TH+ neurons per animal. n=7-9 animals per group. Data are mean ± SEM. *, $p<0.05$; ***, $p<0.001$; ns, not significant. Welch's t test.

PaVN dopaminergic neurons co-express Vesicular Glutamate Transporter 2 (VGLUT2)

Neurotransmitter co-expression and co-release have been reported in many areas of the adult mammalian brain (O'Malley et al., 1992; Gutierrez et al., 2003; Hnasko and Edwards, 2012; Saunders et al., 2015; Zhang et al., 2015). Previous studies of neurotransmitter expression patterns in the PaVN have revealed co-expression of a myriad of neuropeptides (Simmons and Swanson, 2009). However, transmitter co-expression of dopamine with classical neurotransmitters, such as glutamate, has yet to be examined in the PaVN. VGLUT2 is the dominant form of synaptic transporter for glutamatergic neurons in the hypothalamus and midbrain. Additionally, co-expression of TH and VGLUT2 has been reported in ventral tegmental area (VTA) and posterior hypothalamus in rats (Kawano et al., 2006; Zhang et al., 2015). Here we performed immunostaining of TH and VGLUT2 to examine the co-localization of the two proteins in the same cell bodies in the PaVN of animals maintained on the 12L:12D light-dark cycle (Figure 3A). At the protein level, 50% of dopaminergic neurons co-expressed VGLUT2 (208/418 neurons analyzed). However, TH+/VGLUT2+ neurons constitute only 9% of all neurons expressing VGLUT2 (208/2328 neurons analyzed). Additionally, we used RNAscope, a highly-sensitive fluorescent in situ hybridization method capable of detecting single RNA transcripts, to examine co-occurrence of TH mRNA and VGLUT2 mRNA puncta in the same cell bodies in the PaVN. TH immunostaining was performed along with RNAscope to reliably identify cell boundaries of dopaminergic neurons (Figure 3B). 45% of TH protein+ cell bodies contained both TH mRNA and VGLUT2 mRNA puncta in the PaVN (66/148 neurons analyzed), indicating significant co-expression of TH and VGLUT2 at the mRNA level.

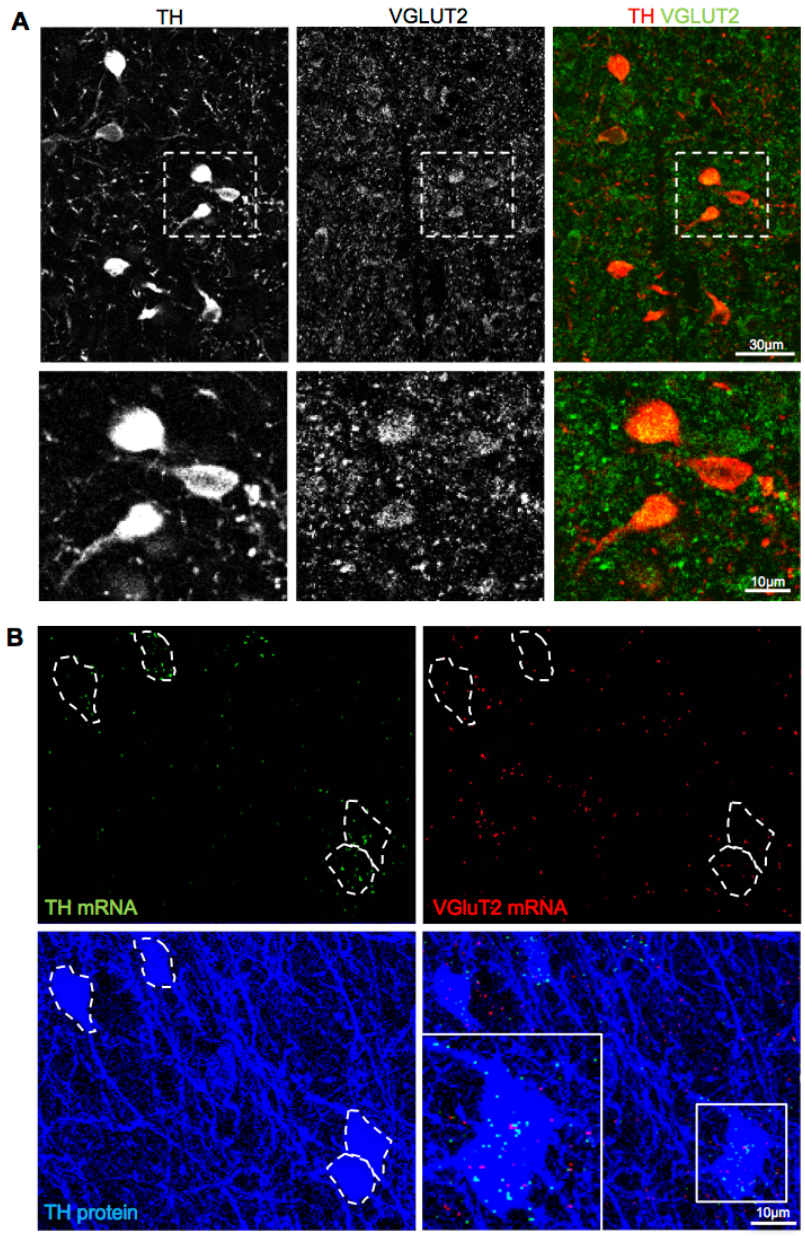

Figure 2.3: PaVN dopaminergic neurons co-express vesicular glutamate transporter VGLUT2. (A) Brain sections from WT rats maintained on 12L:12D were used for Immunofluorescent staining of TH and VGLUT2. From left to right: TH, VGluT2, TH/VGLUT2 co-localization with TH in red and VGLUT2 in green. Top: Low magnification confocal images of many PaVN neurons. Bottom: High magnification view of cell bodies of individual PaVN neurons. TH and VGLUT2 co-localize in the same cell bodies on the left. The neuron on the right expresses only TH. (B) Brain sections from WT rats maintained on 12L:12D were used for RNAscope fluorescent in situ hybridization of TH and VGLUT2 mRNAs combined with immunofluorescent staining of TH. Confocal images of individual channels and merged view are shown. Top left: TH mRNA puncta in green. Top right: VGLUT2 puncta in red. Bottom left: TH protein staining in blue. Bottom right: Merged view of all 3 channels. White dashed lines indicate cell bodies of PaVN TH protein+ neurons. Several TH mRNA puncta and VGLUT2 mRNA puncta are within the boundary of each TH protein+ cell body.

Suppressing activity in excitatory neurons decreases the number of dopaminergic neurons

Because a significant proportion of dopaminergic neurons are also glutamatergic in the PaVN, we investigated whether manipulating neuronal activity of PaVN glutamatergic neurons would change the expression of TH. To suppress the activity of PaVN excitatory glutamatergic neurons, AAV-DIO-Kir was injected together with a Cre-expressing AAV virus under the CaMKII promoter (AAV-CaMKII-Cre) (Dittgen et al., 2004). AAV-DIO-Kir was replaced with AAV-DIO-EYFP in the control group. Animals were maintained on a 12L:12D cycle throughout the experiment. Kir expression decreased the number of PaVN c-Fos+ cells in excitatory neurons, indicating a reduction in neuronal activity in the PaVN (Figure 5 A,B). A significant decrease in the number of PaVN TH+ neurons was observed in the CaMKII-Kir group compared to the control (Figure 4A,B), indicating that suppressing activity of excitatory neurons decreases the number of PaVN dopaminergic neurons.

To rule out the possibility that cell death has contributed to the decreased number of dopaminergic neurons, the TUNEL assay was performed to detect apoptotic cells and NeuN staining was used to quantify the number of neurons and neuronal density in the PaVN. There was no significant difference in the percentage of TUNEL+ cells in the activity suppression group compared to control (Figure 5C,D). In addition, both Kir and EYFP groups showed a similar number of NeuN+ cells, and NeuN+ cell density remained that same in the PaVN (Figure 5E-G). These results indicate that suppressing activity of PaVN excitatory neurons does not increase apoptosis in the PaVN.

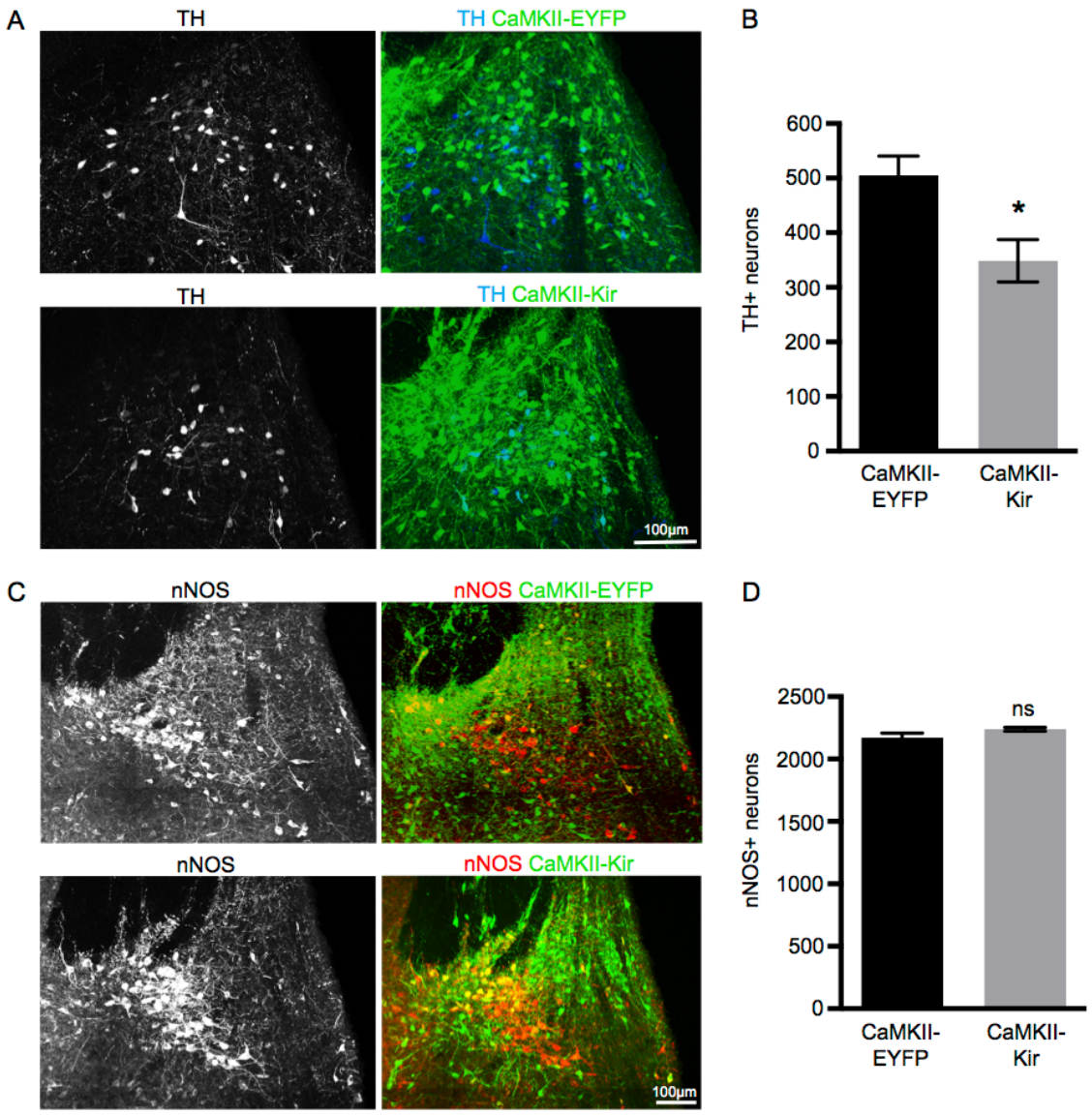

Figure 2.4: Suppressing activity of excitatory neurons decreases the number of dopaminergic neurons in the PaVN after 12L:12D without changing the number of NO neurons. WT rats were injected with AAV-CaMKII-Cre together with AAV-DIO-hKir2.1 in the PaVN. AAV-DIO-hKir2.1 was replaced with AAV-DIO-EYFP in the control group. Animals were kept on 12L:12D after injection. Immunofluorescent staining of TH and nNOS was performed. (A) Confocal images of PaVN TH expression (left) and the expression of TH and viruses (right). (B) Quantification of the number of PaVN TH+ neurons per animal. n=6 animals per group. Data are mean ± SEM. *, $p<0.05$. Welch's t test. (C) Confocal images of PaVN nNOS expression (left) and the expression of nNOS and viruses (right). (D) Quantification of the number of PaVN nNOS+ neurons per animal. n=4-5 animals per group. Data are mean ± SEM. ns, not significant. Welch's t test.

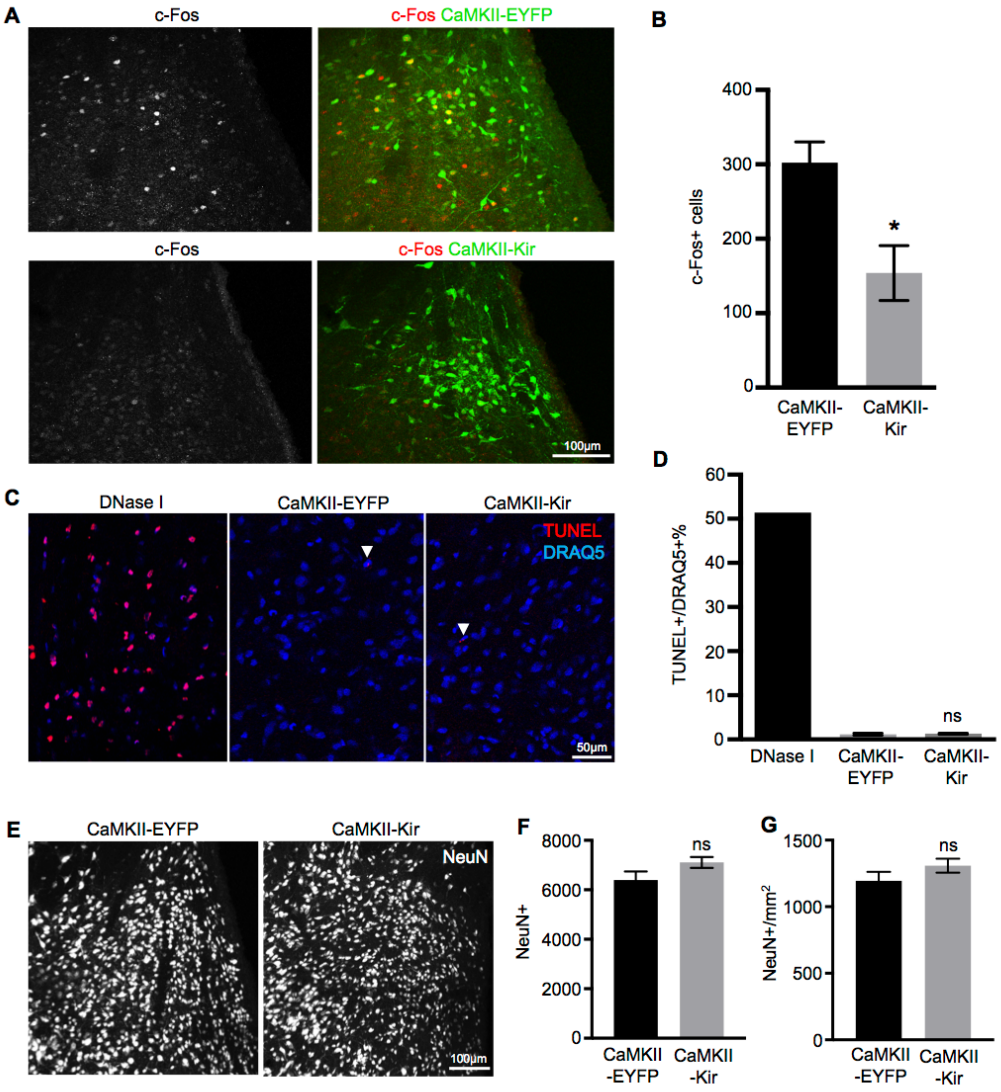

Figure 2.5: Characterization of neuronal activity and cell survival after suppressing activity of PaVN excitatory neurons. The PaVN of WT rats was injected with AAV-CaMKII-Cre together with AAV-DIO-hKir2.1. AAV-DIO-EYFP was used as control. Animals were kept on 12L:12D after injection. (A) Immunofluorescent staining of c-Fos was performed. Confocal images show PaVN c-Fos expression (left) and the expression of c-Fos and viruses (right). (B) Quantification of the number of PaVN c-Fos+ neurons per animal. n=5-6 animals per group. Data are mean ± SEM. *, $p<0.05$. Welch's t test. (C) The TUNEL assay was used to detect cell death in brain sections from animals expressing these viruses. Sections treated with DNase I were used as positive controls. Confocal images from different conditions show TUNEL+ signal in red and DRAQ5 DNA staining in blue. From left to right: Positive control, CaMKII-EYFP, CaMKII-Kir. White arrowheads indicate TUNEL+ cells in the experimental groups. (D) Quantification of the TUNEL assay showing the percentage of TUNEL+ cells in 3 conditions. n=3 animals per group. Data are mean ± SEM. ns, not significant. Welch's t test. (E) Confocal images showing PaVN NeuN immunostaining from different groups. Left: CaMKII-EYFP. Right: CaMKII-Kir. (F) Quantification of the number of PaVN NeuN+ cells per animal. n=3-4 animals per group. Data are mean ± SEM. ns, not significant. Welch's t test. (G) Quantification of the number of PaVN NeuN+ cells per mm^2. n=3-4 animals per group. Data are mean ± SEM. ns, not significant. Welch's t test.

To test the specificity of the decrease in PaVN TH+ neurons, we investigated whether suppressing activity of excitatory neurons affects other neuronal types in the PaVN. Nitric Oxide (NO) is another neurotransmitter expressed in the PaVN that can be easily detected by immunostaining its synthetic enzyme, neuronal nitric oxide synthase (nNOS). nNOS expression and enzymatic activity have been shown to be regulated by NMDA receptor activation, Ca^{2+} influx, and CaMKII activity (Rameau et al., 2007). The number of NO neurons has been shown to be altered in patients and animal models of stress and depressive disorders (Kishimoto et al., 1996; Bernstein et al., 1998; Gao et al., 2014). nNOS+ neurons and TH+ neurons are intermingled populations in the PaVN but nNOS and TH do not co-express in the same neurons (data not shown). There is no difference in the number of PaVN nNOS+ neurons between the CaMKII-Kir and CaMKII-EYFP groups (Figure 4C,D), suggesting that suppressing activity of PaVN excitatory neurons does not change the number of PaVN NO neurons. These results provide evidence for specificity of the effect of suppressing activity of excitatory neurons.

We then tested whether the decrease in the number of dopaminergic neurons is caused by decreased neuronal activity of glutamatergic neurons specifically, or a decrease in overall neuronal activity in the PaVN. Globally suppressing PaVN neuronal activity was achieved by injecting AAV-DIO-Kir coupled with a Cre-expressing AAV virus under the Synapsin promoter (AAV-Syn-Cre) (Kugler et al., 2003). Kir expression caused a decrease in the number of c-Fos+ cells in the PaVN of animals maintained on a 12L:12D cycle (Figure 6 A,B). However, there is no difference in the number of TH+ neurons between Syn-Kir and Syn-EYFP groups (Figure 6 A,C). This result suggests that the decreased

number of dopaminergic neurons is caused specifically by suppressing neuronal activity of glutamatergic neurons in the PaVN.

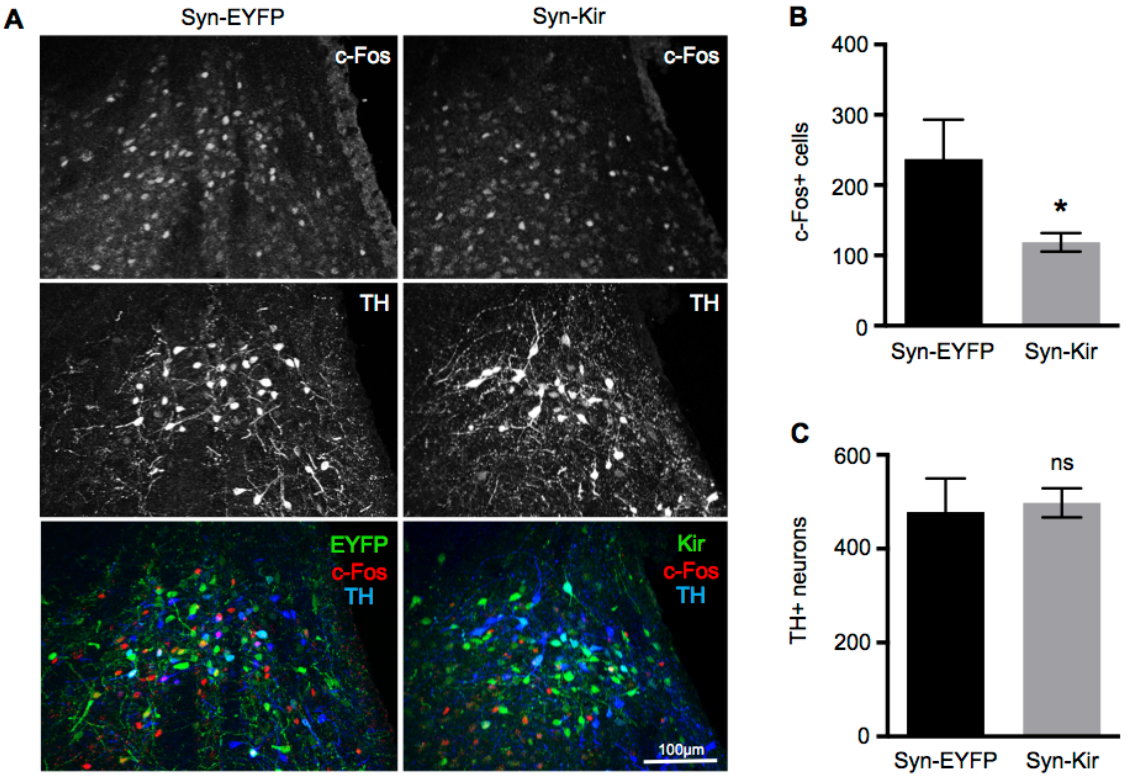

Figure 2.6: Suppressing overall neuronal activity does not affect the number of dopaminergic neurons in the PaVN after 12L:12D. WT rats were injected with AAV-Synapsin-Cre together with AAV-DIO-hKir2.1 in the PaVN. AAV-DIO-EYFP was used as control. Animals were maintained on 12L:12D after injection. Immunofluorescent staining of TH and c-Fos was performed. (A) Confocal images show PaVN c-Fos expression (top), TH expression (middle), and the expression of c-Fos, TH and viruses (bottom). The control group (Syn-EYFP) is shown on the left and the experimental group (Syn-Kir) is shown on the right. (B) Quantification of the number of PaVN c-Fos+ neurons per animal. n=5-10 animals per group. Data are mean ± SEM. *, $p<0.05$. Welch's t test. (C) Quantification of the number of PaVN TH+ neurons per animal. n=5-10 animals per group. Data are mean ± SEM. ns, not significant. Welch's t test.

DISCUSSION

Light-induced neuronal activation of PaVN dopaminergic neurons

The ventrolateral SCN receives retinal projections from the direct retinohypothalamic tract and indirect geniculohypothalamic tract, and entrains internal

circadian oscillation to external light-dark cycle (Moore, 1983; Moore et al., 1995; Moore, 1996). These photic signals induce rhythmic c-Fos expression in the SCN (Aronin et al., 1990; Kornhauser et al., 1990; Earnest and Olschowka, 1993). The PaVN receives direct input from light-sensitive SCN neurons (Watts et al., 1987; Vrang et al., 1995b; Munch et al., 2002). Therefore, it is reasonable to hypothesize that the activity of PaVN neurons changes after exposure to different photoperiods and that this change can be detected by c-Fos immunoreactivity.

Our results indicate that during the balanced-day photoperiod, c-Fos activity in the overall neuronal population and in the dopaminergic neurons can be detected in the PaVN when examined 3-4 hours after the onset of the light phase, reflecting a moderate light-induced activation of the PaVN at the baseline level. During long-day photoperiod exposure, c-Fos activity of both the dopaminergic neurons and the total PaVN neuronal population is much higher compared to activity resulting from exposure to the balanced-day, indicating elevated neuronal activation following extended light phase exposure. Elevated PaVN c-Fos activity can be detected after 4 days of long-day photoperiod, prior to detectable changes in neurotransmitter expression or anxiety and depression-like behaviors, all of which occur after a week of long-day photoperiod exposure. Given the temporal sequence of the changes, it is most likely that altered long-day photoperiod leads to elevated PaVN c-Fos activity directly through the efferent projections from SCN to PaVN, which in turn results in transmitter switching and changes in behavior. Suppressing the elevation of dopaminergic neuronal activity during the long-day photoperiod blocks their transmitter switch, providing further support for this argument.

Future work will determine the temporal dynamics of PaVN c-Fos activation to learn whether the observed elevation in neuronal activity is transient or sustained over the course of 2 weeks of photoperiod exposure. Additionally, it will be important to investigate whether PaVN dopaminergic neurons receive direct monosynaptic projections from SCN retinorecipient neurons or multisynaptic connections through other SCN and PaVN neurons.

Cell-autonomous mechanism of neurotransmitter switching in the adult brain

Many forms of neuroplasticity are regulated by neuronal activity through either cell-autonomous or non-cell-autonomous mechanisms (Spitzer, 2006). On one hand, it is well established that elevated intracellular Ca^{2+} following depolarization serves as a second messenger and can cause transcriptional and translational changes of neurotransmitter synthetic enzymes, receptors, and ion channels of the same neurons directly. On the other hand, cell secretion and cell-cell surface signaling can be regulated by neuronal activity and affect intracellular signaling of neighboring neurons non-cell-autonomously.

In the developing *Xenopus* spinal cord, where neurotransmitter re-specification or switching was first described, the mechanism through which neuronal activity regulates this novel form of neuroplasticity is non-cell-autonomous. Globally suppressing neuronal activity of all spinal neurons by Kir overexpression in vitro and in vivo cause transmitter re-specification from GABA to glutamate to restore homeostasis. However, Kir expression sparsely in individual spinal neurons does not change their probability of becoming glutamatergic or GABAergic (Borodinsky et al., 2004; Guemez-Gamboa et al., 2014). Secretion of BDNF mediates this non-cell-autonomous activity-dependent process of transmitters switching in the developing nervous system (Guemez-Gamboa et al., 2014).

In the present study of neurotransmitter switching of PaVN dopaminergic neurons in the adult rat brain, both PaVN dopaminergic neuronal activity and overall PaVN neuronal activity increase after long-day photoperiod exposure prior to transmitter switching. Our results indicate that suppressing activity of the population of dopaminergic neurons by Kir expression in TH-Cre rats is sufficient to block their transmitter switch in response to exposure to the long-day photoperiod, potentially suggesting a cell-population-autonomous mechanism. It would be challenging to test whether manipulating activity of single dopaminergic neurons will change their likelihood of switching transmitters after long-day exposure in vivo. Theoretically, sparse infection of dopaminergic neurons by either Kir or control virus, followed by long-day exposure, could address whether manipulating activity of single dopaminergic neurons changes transmitters. If single Kir-infected dopaminergic neurons are more likely to remain TH+ after long-day exposure than control, then dopaminergic neuronal activity is also required for transmitter switching at the single cell level. However, with the only currently available TH-Cre transgenic line targeting dopaminergic neurons in rats, ~20% of PaVN virus-infected neurons do not express a detectable level of TH protein. This could reflect the highly plastic and variable nature of TH expression in the PaVN since we frequently observe PaVN neurons that are TH mRNA+ but TH protein-. Given the relatively small decrease (~30%) in the number of TH+ neurons after long-day photoperiod exposure, the "off-target" labeling in TH-Cre rats will introduce significant noise to the sparse infection approach and render it ineffective. In summary, transmitter switching as assayed in these experiments is cell-population-autonomous; whether it is individual-cell-autonomous remains to be tested.

Neurotransmitter co-expression and neurotransmitter switching

VTA neurons can co-express both TH and VGLUT2 in their cell bodies in vitro and in vivo (Sulzer et al., 1998; Dal Bo et al., 2004; Kawano et al., 2006). Additionally, axons from VTA dopaminergic neurons contain TH, VMAT, and VGLUT2, and co-release both dopamine and glutamate in the nucleus accumbens (Sulzer et al., 1998; Hnasko et al., 2010; Zhang et al., 2015). Here we have demonstrated co-expression of TH and VGLUT2 in the cell bodies of PaVN dopaminergic neurons both at the mRNA and at the protein level.

Transmitter switching and transmitter co-expression and co-release appear to be intrinsically linked biological processes: on one hand, neurons that normally co-express two or more neurotransmitters can up- or down-regulate their transmitters differentially under specific circumstances and give rise to functional neurotransmitter switching. On the other hand, when examined at fixed time points, neurons in the process of switching their major neurotransmitter would appear to be expressing markers for multiple neurotransmitters at the same time. Future work will quantify the number of PaVN VGLUT2+ and TH+/VGLUT2+ neurons after long-day photoperiod exposure. This will determine whether PaVN dopaminergic neurons maintain, downregulate or upregulate their VGLUT2 expression in the process of losing their TH expression after long-day exposure.

The functional implication of PaVN TH/VGLUT2 co-expression in regulating stress and anxiety responses achieved by the release of CRF remains to be investigated. Most PaVN CRF neurons do not receive direct input from SCN, suggesting that photoperiods influence the release of CRF mostly through a multi-synaptic pathway (Vrang

et al., 1995a). PaVN CRF neurons express both excitatory glutamate receptors and the D2 inhibitory dopamine receptor (Aubry et al., 1996; Dulcis et al., 2013). Additionally, the number of glutamatergic synapses and the level of glutamate receptors on the CRF neurons have been shown to increase after exposure to acute and chronic stressors (Flak et al., 2009; Bains et al., 2015). Removal of inhibitory input seems to be necessary for the activation of PaVN CRF neurons in addition to increased glutamate release (Cole and Sawchenko, 2002). Downregulation of inhibitory dopamine release from the same axons that co-release excitatory glutamate on CRF neurons may facilitate release of CRF, contributing to the increased stress and anxiety behaviors observed following exposure to long-day photoperiods.

Transmitter switching in disease

Neurotransmitter imbalance and dysregulation have been implicated in many common neurological and psychiatric disorders, such as Parkinson's disease and schizophrenia (Damier et al., 1999; Howes et al., 2012; Howes and Murray, 2014). Additionally, dysfunction of many classic neuroplasticity mechanisms, in which the brain adjusts inappropriately in response to extreme environmental stimuli, has been thought to increase susceptibility to psychiatric disorders. For example, many people experience traumatic events in their lifetime but only a small fraction of them develop post-traumatic stress disorder (PTSD), indicating impaired regulation of fear and anxiety responses (Hill and Martinowich, 2016).

We have investigated the mechanism of transmitter switching of dopaminergic neurons in a specialized disease model, in which altered photoperiod leads to anxiety and depression-like behaviors in rats, mimicking seasonal affective disorder in humans.

Further work will examine the prevalence of transmitter switching in more generalized models of stress-related illnesses and other mood disorders. Many effective treatments for diseases of the nervous system have been shown to induce plasticity-related structural and functional changes in the brain (Davidson and McEwen, 2012). Moreover, neurotransmitter synthetic enzymes and receptors are promising targets for pharmaceutical agents treating neurological and psychiatric disorders. Characterization of transmitter switching in animal models of disease and knowledge gained from studying this newly recognized form of neuronal plasticity may lead to development of novel diagnostic and therapeutic tools for patients.

EXPERIMENTAL PROCEDURES

Animal Use

All animal procedures were performed in accordance with institutional guidelines and approved by the UCSD Institutional Animal Care and Use Committee. Female TH-Cre Long-Evans rats were generously provided by Dr. Karl Deisseroth. The rat colony was maintained by breeding heterozygous female TH-Cre rats with male wild-type Long-Evans rats from a commercial source (Charles River Laboratories). The offspring were genotyped using the following primers: Cre-F AAGAACCTGATGGACATGTTCAGGGATCG, Cre-R CCACCGTCAGTACGTGAGATATCTTTAACC (Witten et al., 2011). 8-week old male TH-Cre offspring and their wild-type littermates were used in the study. Rats were group-housed with food and water *ad libitum* on a standard 12 h light/12 h dark schedule (light on at 7 am) prior to any experimental procedures. For balanced-day (12L:12D) and

long-day photoperiod (19L:5D) exposure, animals were single-housed in the custom-made photo-chambers for the indicated amount of time.

Virus Injection

8-week old male rats were anesthetized with isoflurane during stereotaxic injection using a stereotaxic apparatus (David Kopf Instruments) and Hamilton syringe (7647-1) and needle (33 gauge, 7762-06). The anterior PaVN (Bregma AP -0.8, ML +0.8, DV -7.2, -7.0) was targeted and a total of 1 µl of viral vector was injected into the PaVN unilaterally. The needle was left in place for 5 minutes after each injection. Serial dilutions of viral vectors were tested in WT and TH-Cre rats and the lowest titers with >50% infection rate after 4 weeks were chosen for experiments. The vendors and final physical titers of viral vectors are as follows: AAVdj-CMV-DIO-Kir2.1-zsGreen (Stanford viral core/ Deisseroth lab), 3-5 x 10^{13} GC/mL; AAVdj-EF1a-DIO-EYFP (Deisseroth lab), 6-10 x 10^{12} GC/mL; AAV1-hSyn-Cre-WPRE-hGH (U Penn viral core), 2.5 x 10^{12} GC/mL; AAV9-CaMKII0.4-Cre-SV40 (U Penn viral core), 1.8 x 10^{13} GC/mL.

Immunofluorescent Staining and Confocal Imaging

At 10 am-1 pm during the light cycle rats were deeply anesthetized with pentobarbital sodium and perfused transcardially with 200 ml of 1×PBS followed by 200 ml of 4% paraformaldehyde (PFA) in 1xPBS. Brains were then removed and post-fixed in 4% PFA 1xPBS at 4°C overnight followed by 30% sucrose for 4-5 days at 4°C until the brains sank. For immunofluorescent staining, 40 µm coronal sections were cut with a microtome and every third section of the anterior PaVN was used for staining. Sections were incubated with a blocking solution (5% horse serum or 2% bovine serum albumin in 1x PBS with 0.3% Triton-X 100) for 2 hours at room temperature (RT) and then incubated

at 4°C in the blocking solution with primary antibodies overnight. After rinsing in 1xPBS 3 times, 10 minutes each time, sections were incubated in the blocking solution with secondary antibodies at RT for 2 hours. Sections were then rinsed, mounted on glass slides with 2% gelatin, and coverslipped using for Fluoromount-G (Southern Biotech) or ProLong Gold Antifade Mountant (Life Technologies).

The following primary antibodies were used: Mouse anti-TH (Millipore MAB318), 1:200; Rabbit anti-TH (Millipore AB152), 1:500; Mouse anti-VGLUT2 (Millipore MAB5504), 1:100; Goat anti-c-Fos (Santa Cruz SC-52-G), 1:250; Rabbit anti-nNOS (Life Technologies 61-7000), 1:500; Mouse anti-NeuN (Millipore MAB377), 1:500; Guinea pig anti-GFP (Synaptic Systems 132005), 1:4000. The following Alexa Fluor IgG secondary antibodies were used: 488 Donkey anti-Guinea pig, 488 Donkey anti-rabbit, 555 Donkey anti-Goat, 555 Donkey anti-rabbit, 647 Donkey anti-mouse (Life Technologies or Jackson ImmunoResearch), 1:300.

A Leica SP5 confocal microscope with a 25x/0.95 water-immersion objective was used to acquire all fluorescent images.

RNAscope In Situ Hybridization

RNAscope Multiplex Fluorescent Reagent Kit (Advanced Cell Diagnostics, 320850) and Target Probes for rat TH mRNA (Advanced Cell Diagnostics, 314651-C2) and rat VGLUT2 (Slc17a6) mRNA (Advanced Cell Diagnostics, 317011-C1) were used. The experiment was performed according to manufacturer's instructions. In a RNAase-free environment, 20 μm fixed brain sections were mounted on a glass slide immediately after microtome sectioning and baked in a 60°C dry oven for 30 minutes. Sections were rehydrated in PBS for 5 minutes before a 5-minute incubation in 1x Target Retrieval

solution at 90-95°C. Sections were then rinsed with distilled water and 100% EtOH. Subsequently, sections were incubated with the following solutions in the HybEZTM humidified Oven at 40°C with rinsing steps in between: Protease III 30 minutes, Target Probes 2 hours, Amp 1-FL 30 minutes, Amp 2-FL 15 minutes, Amp 3-FL 30 minutes, and Amp 4-FL 15 minutes. Afterwards, standard immunofluorescent staining was performed using Rabbit anti-TH (Millipore AB152, 1:500) to detect TH protein in the same sections.

TUNEL Assay

An In Situ Cell Death Detection (TUNEL) Kit, TMR Red (ROCHE 12156792910) was used. PFA-fixed brain sections were mounted and dried on glass slides. After rehydration in 1x PBS for 5 minutes, sections were re-fixed with 1% PFA for 20 minutes at RT before rinsing in 1xPBS 3 times, 5 minutes each time. Sections were then incubated in freshly prepared permeabilization solution (0.1% sodium citrate and 1% Triton X-100) for 1 hour at RT. After rinsing, sections were incubated with TUNEL reaction mixture (250 µl per section, 25 µl TdT solution + 225 µl label solution) in a humidified chamber for 3 hours at 37°C in the dark. The sections were rinsed and mounted with DRAQ5-flurormount. The positive control was treated with DNase I (NEB, 10U/ml) for 1 hour at 37°C before the TUNEL reaction.

Cell Number and Cell Density Quantification

For c-Fos, TH, nNos, TUNEL, and DRAQ5 quantification, 3D fluorescent confocal image stacks were used to manually count the number of cell bodies using the Leica Application Suite X software. For NeuN and NeuN density, 3D fluorescent confocal image stacks were quantified with ImageJ software using the 3D objects counter and area measurement functions.

Statistics

Statistical analyses were performed using Prism 7 software. Means and SEMs were reported for all experiments. For comparisons between two groups, Welch's t test was used. For comparisons of more than two groups, one-way ANOVA followed by Tukey's multiple comparisons test was used. Values were considered significantly different at $p < 0.05$.

ACKNOWLEDGMENTS

We thank Dr. Stefan Leutgeb and Dr. Karl Deisseroth for providing critical reagents, tools and space for our experiments. We thank Dr. Hui-quan Li for technical support of the RNAscope experiment. This work is supported by an HHMI International Predoctoral Fellowship to D.M. and Ellison Medical Foundation and W.M. Keck Foundation grants to N.C.S.

Chapter 2, in full, is currently being prepared for submission for publication of the material. Meng D, Spitzer NC. Neuronal activity regulates transmitter switching in the adult brain. The dissertation author was the primary investigator and author of this material.

REFERENCES

Aronin, N., Sagar, S.M., Sharp, F.R., and Schwartz, W.J. (1990). Light regulates expression of a Fos-related protein in rat suprachiasmatic nuclei. Proc Natl Acad Sci U S A *87*, 5959-5962.

Aubry, J.M., Bartanusz, V., Pagliusi, S., Schulz, P., and Kiss, J.Z. (1996). Expression of ionotropic glutamate receptor subunit mRNAs by paraventricular corticotropin-releasing factor (CRF) neurons. Neurosci Lett *205*, 95-98.

Bains, J.S., Wamsteeker Cusulin, J.I., and Inoue, W. (2015). Stress-related synaptic plasticity in the hypothalamus. Nat Rev Neurosci *16*, 377-388.

Bernstein, H.G., Stanarius, A., Baumann, B., Henning, H., Krell, D., Danos, P., Falkai, P., and Bogerts, B. (1998). Nitric oxide synthase-containing neurons in the human hypothalamus: reduced number of immunoreactive cells in the paraventricular nucleus of depressive patients and schizophrenics. Neuroscience *83*, 867-875.

Borodinsky, L.N., Root, C.M., Cronin, J.A., Sann, S.B., Gu, X., and Spitzer, N.C. (2004). Activity-dependent homeostatic specification of transmitter expression in embryonic neurons. Nature *429*, 523-530.

Buijs, R.M., Markman, M., Nunes-Cardoso, B., Hou, Y.X., and Shinn, S. (1993). Projections of the suprachiasmatic nucleus to stress-related areas in the rat hypothalamus: a light and electron microscopic study. J Comp Neurol *335*, 42-54.

Bullitt, E. (1990). Expression of c-fos-like protein as a marker for neuronal activity following noxious stimulation in the rat. J Comp Neurol *296*, 517-530.

Christoffel, D.J., Golden, S.A., and Russo, S.J. (2011). Structural and synaptic plasticity in stress-related disorders. Rev Neurosci *22*, 535-549.

Cole, R.L., and Sawchenko, P.E. (2002). Neurotransmitter regulation of cellular activation and neuropeptide gene expression in the paraventricular nucleus of the hypothalamus. J Neurosci *22*, 959-969.

Dal Bo, G., St-Gelais, F., Danik, M., Williams, S., Cotton, M., and Trudeau, L.E. (2004). Dopamine neurons in culture express VGLUT2 explaining their capacity to release glutamate at synapses in addition to dopamine. J Neurochem *88*, 1398-1405.

Damier, P., Hirsch, E.C., Agid, Y., and Graybiel, A.M. (1999). The substantia nigra of the human brain. II. Patterns of loss of dopamine-containing neurons in Parkinson's disease. Brain *122 (Pt 8)*, 1437-1448.

Davidson, R.J., and McEwen, B.S. (2012). Social influences on neuroplasticity: stress and interventions to promote well-being. Nat Neurosci *15*, 689-695.

Destexhe, A., and Marder, E. (2004). Plasticity in single neuron and circuit computations. Nature *431*, 789-795.

Dittgen, T., Nimmerjahn, A., Komai, S., Licznerski, P., Waters, J., Margrie, T.W., Helmchen, F., Denk, W., Brecht, M., and Osten, P. (2004). Lentivirus-based genetic manipulations of cortical neurons and their optical and electrophysiological monitoring in vivo. Proc Natl Acad Sci U S A *101*, 18206-18211.

Dulcis, D., Jamshidi, P., Leutgeb, S., and Spitzer, N.C. (2013). Neurotransmitter switching in the adult brain regulates behavior. Science *340*, 449-453.

Earnest, D.J., and Olschowka, J.A. (1993). Circadian regulation of c-fos expression in the suprachiasmatic pacemaker by light. J Biol Rhythms *8 Suppl*, S65-71.

Engert, F., and Bonhoeffer, T. (1999). Dendritic spine changes associated with hippocampal long-term synaptic plasticity. Nature *399*, 66-70.

Flak, J.N., Ostrander, M.M., Tasker, J.G., and Herman, J.P. (2009). Chronic stress-induced neurotransmitter plasticity in the PVN. J Comp Neurol *517*, 156-165.

Gao, S.F., Lu, Y.R., Shi, L.G., Wu, X.Y., Sun, B., Fu, X.Y., Luo, J.H., and Bao, A.M. (2014). Nitric oxide synthase and nitric oxide alterations in chronically stressed rats: a model for nitric oxide in major depressive disorder. Psychoneuroendocrinology *47*, 136-140.

Gu, X., and Spitzer, N.C. (1995). Distinct aspects of neuronal differentiation encoded by frequency of spontaneous Ca2+ transients. Nature *375*, 784-787.

Guemez-Gamboa, A., Xu, L., Meng, D., and Spitzer, N.C. (2014). Non-cell-autonomous mechanism of activity-dependent neurotransmitter switching. Neuron *82*, 1004-1016.

Gutierrez, R., Romo-Parra, H., Maqueda, J., Vivar, C., Ramirez, M., Morales, M.A., and Lamas, M. (2003). Plasticity of the GABAergic phenotype of the "glutamatergic" granule cells of the rat dentate gyrus. J Neurosci *23*, 5594-5598.

Hill, J.L., and Martinowich, K. (2016). Activity-dependent signaling: influence on plasticity in circuits controlling fear-related behavior. Curr Opin Neurobiol *36*, 59-65.

Hnasko, T.S., Chuhma, N., Zhang, H., Goh, G.Y., Sulzer, D., Palmiter, R.D., Rayport, S., and Edwards, R.H. (2010). Vesicular glutamate transport promotes dopamine storage and glutamate corelease in vivo. Neuron *65*, 643-656.

Hnasko, T.S., and Edwards, R.H. (2012). Neurotransmitter corelease: mechanism and physiological role. Annu Rev Physiol *74*, 225-243.

Howes, O.D., Kambeitz, J., Kim, E., Stahl, D., Slifstein, M., Abi-Dargham, A., and Kapur, S. (2012). The nature of dopamine dysfunction in schizophrenia and what this means for treatment. Arch Gen Psychiatry *69*, 776-786.

Howes, O.D., and Murray, R.M. (2014). Schizophrenia: an integrated sociodevelopmental-cognitive model. Lancet *383*, 1677-1687.

Kawano, M., Kawasaki, A., Sakata-Haga, H., Fukui, Y., Kawano, H., Nogami, H., and Hisano, S. (2006). Particular subpopulations of midbrain and hypothalamic dopamine neurons express vesicular glutamate transporter 2 in the rat brain. J Comp Neurol *498*, 581-592.

Kishimoto, J., Tsuchiya, T., Emson, P.C., and Nakayama, Y. (1996). Immobilization-induced stress activates neuronal nitric oxide synthase (nNOS) mRNA and protein in hypothalamic-pituitary-adrenal axis in rats. Brain Res *720*, 159-171.

Kornhauser, J.M., Nelson, D.E., Mayo, K.E., and Takahashi, J.S. (1990). Photic and circadian regulation of c-fos gene expression in the hamster suprachiasmatic nucleus. Neuron *5*, 127-134.

Kubo, Y., Baldwin, T.J., Jan, Y.N., and Jan, L.Y. (1993). Primary structure and functional expression of a mouse inward rectifier potassium channel. Nature *362*, 127-133.

Kugler, S., Kilic, E., and Bahr, M. (2003). Human synapsin 1 gene promoter confers highly neuron-specific long-term transgene expression from an adenoviral vector in the adult rat brain depending on the transduced area. Gene Ther *10*, 337-347.

Marder, E., and Goaillard, J.M. (2006). Variability, compensation and homeostasis in neuron and network function. Nat Rev Neurosci *7*, 563-574.

Moore, R.Y. (1983). Organization and function of a central nervous system circadian oscillator: the suprachiasmatic hypothalamic nucleus. Fed Proc *42*, 2783-2789.

Moore, R.Y. (1996). Entrainment pathways and the functional organization of the circadian system. Prog Brain Res *111*, 103-119.

Moore, R.Y., Speh, J.C., and Card, J.P. (1995). The retinohypothalamic tract originates from a distinct subset of retinal ganglion cells. J Comp Neurol *352*, 351-366.

Munch, I.C., Moller, M., Larsen, P.J., and Vrang, N. (2002). Light-induced c-Fos expression in suprachiasmatic nuclei neurons targeting the paraventricular nucleus of the hamster hypothalamus: phase dependence and immunochemical identification. J Comp Neurol *442*, 48-62.

O'Malley, D.M., Sandell, J.H., and Masland, R.H. (1992). Co-release of acetylcholine and GABA by the starburst amacrine cells. J Neurosci *12*, 1394-1408.

Rameau, G.A., Tukey, D.S., Garcin-Hosfield, E.D., Titcombe, R.F., Misra, C., Khatri, L., Getzoff, E.D., and Ziff, E.B. (2007). Biphasic coupling of neuronal nitric oxide synthase phosphorylation to the NMDA receptor regulates AMPA receptor trafficking and neuronal cell death. J Neurosci *27*, 3445-3455.

Saunders, A., Granger, A.J., and Sabatini, B.L. (2015). Corelease of acetylcholine and GABA from cholinergic forebrain neurons. Elife *4*.

Simmons, D.M., and Swanson, L.W. (2009). Comparison of the spatial distribution of seven types of neuroendocrine neurons in the rat paraventricular nucleus: toward a global 3D model. J Comp Neurol *516*, 423-441.

Spitzer, N.C. (2006). Electrical activity in early neuronal development. Nature *444*, 707-712.

Spitzer, N.C. (2015). Neurotransmitter Switching? No Surprise. Neuron *86*, 1131-1144.

Sulzer, D., Joyce, M.P., Lin, L., Geldwert, D., Haber, S.N., Hattori, T., and Rayport, S. (1998). Dopamine neurons make glutamatergic synapses in vitro. J Neurosci *18*, 4588-4602.

Turrigiano, G.G. (2008). The self-tuning neuron: synaptic scaling of excitatory synapses. Cell *135*, 422-435.

Vrang, N., Larsen, P.J., and Mikkelsen, J.D. (1995a). Direct projection from the suprachiasmatic nucleus to hypophysiotrophic corticotropin-releasing factor immunoreactive cells in the paraventricular nucleus of the hypothalamus demonstrated by means of Phaseolus vulgaris-leucoagglutinin tract tracing. Brain Res *684*, 61-69.

Vrang, N., Larsen, P.J., Moller, M., and Mikkelsen, J.D. (1995b). Topographical organization of the rat suprachiasmatic-paraventricular projection. J Comp Neurol *353*, 585-603.

Watts, A.G., Swanson, L.W., and Sanchez-Watts, G. (1987). Efferent projections of the suprachiasmatic nucleus: I. Studies using anterograde transport of Phaseolus vulgaris leucoagglutinin in the rat. J Comp Neurol *258*, 204-229.

Witten, I.B., Steinberg, E.E., Lee, S.Y., Davidson, T.J., Zalocusky, K.A., Brodsky, M., Yizhar, O., Cho, S.L., Gong, S., Ramakrishnan, C., Stuber G.D., Tye K.M., Janak P.H., Deisseroth K. (2011). Recombinase-driver rat lines: tools, techniques, and optogenetic application to dopamine-mediated reinforcement. Neuron *72*, 721-733.

Zhang, S., Qi, J., Li, X., Wang, H.L., Britt, J.P., Hoffman, A.F., Bonci, A., Lupica, C.R., and Morales, M. (2015). Dopaminergic and glutamatergic microdomains in a subset of rodent mesoaccumbens axons. Nat Neurosci *18*, 386-392.